NASA Contractor Report 159302

DESIGN AND ANALYSIS OF A STIFFENED COMPOSITE FUSELAGE PANEL

J. N. Dickson and S. B. Biggers

LOCKHEED-GEORGIA COMPANY
A Division of Lockheed Corporation
Marietta, Georgia 30063

Contract NAS1-15949
August 1980

National Aeronautics and Space Administration
Langley Research Center
Hampton, Virginia 23665

*MSG D14 DROLS PROCESSING - LAST INPUT IGNORED

-- 1 OF 3
-- ***DTIC DOES NOT HAVE THIS ITEM***
-- 1 - AD NUMBER: D432823
-- 5 - CORPORATE AUTHOR: LOCKHEED-GEORGIA CO MARIETTA
-- 6 - UNCLASSIFIED TITLE: DESIGN AND ANALYSIS OF A STIFFENED
-- COMPOSITE FUSELAGE PANEL,
--10 - PERSONAL AUTHORS: DICKSON,J. N. ;BIGGERS,S. B. ;
--11 - REPORT DATE: AUG , 1980
--12 PAGINATION: 50P
--14 - REPORT NUMBER: LG80ER0137
--15 - CONTRACT NUMBER: NAS1-15949
--18 - MONITOR ACRONYM: NASA
--19 - MONITOR SERIES: CR-159302
--20 - REPORT CLASSIFICATION: UNCLASSIFIED
--22 - LIMITATIONS (ALPHA): APPROVED FOR PUBLIC RELEASE; DISTRIBUTION
-- UNLIMITED. AVAILABILITY: NATIONAL TECHNICAL INFORMATION SERVICE,
-- SPRINGFIELD, VA. 22161. N80-31020.
--33 - LIMITATION CODES: 1

-- END Y FOR NEXT ACCESSION END

Alt-Z FOR HELP3 ANSI 3 HDX 3 3 LOG CLOSED 3 PRINT OFF 3 PARITY

FOREWORD

This report is prepared by the Lockheed-Georgia Company under Contract NAS1-15949, "Advanced Composite Structural Design Technology for Commercial Transport Aircraft," and describes the design and analyses of a stiffened curved fuselage panel performed under Task Assignment No. 1 of the contract. The program is sponsored by the National Aeronautics and Space Administration, Langley Research Center (NASA/LaRC). Dr. James H. Starnes is the Project Engineer for NASA/LaRC. John N. Dickson is the Program Manager for the Lockheed-Georgia Company.

In addition to the authors the following Lockheed specialist/consultants made major contributions to the material presented.

Dr. C. S. Chu	Fail-Safe Analysis
S. D. Higham	Advanced Design
L. W. Liu	Strength Analysis
Dr. J.T.S. Wang (Georgia Tech)	Shell Analysis

TABLE OF CONTENTS

DESIGN AND ANALYSIS OF A STIFFENED COMPOSITE FUSELAGE PANEL

J. N. Dickson
S. B. Biggers
Lockheed-Georgia Company

SUMMARY

A stiffened composite panel has been designed that is representative of the fuselage structure of existing wide bodied aircraft. The panel is a minimum weight design, based on the current level of technology and realistic loads and criteria. Several different stiffener configurations were investigated in the optimization process. The final configuration is an all graphite/epoxy J-stiffened design in which the skin between adjacent stiffeners is permitted to buckle under design loads. Fail-safe concepts typically employed in metallic fuselage structure have been incorporated in the design. A conservative approach has been used with regard to structural details such as skin/frame and stringer/frame attachments and other areas where sufficient design data was not available.

INTRODUCTION

The development of the technology necessary to implement extensive application of composite materials for primary structures of commercial transport aircraft is one of the principal objectives of the National Aeronautics and Space Administration (NASA) as exemplified by the many research and development programs funded in this area. The goal of the Aircraft Energy Efficiency (ACEE) Program is to establish, by 1985, the technological basis for the design of subsonic transport aircraft requiring 40 percent less fuel than current designs. Fuel savings can be accomplished through improved aerodynamics, better engine efficiency and structural weight reductions. The current contract will focus on the latter by assisting NASA in the development of minimum weight design technology for composite primary structures.

To take full advantage of the weight savings potential of advanced composites, optimum structural designs must be provided that satisfy all requirements with respect to structural integrity, stiffness, durability and damage tolerance. At the same time, nonstructural criteria such as ease of manufacturing, producibility and cost must be considered in the design.

Composites require the consideration of different failure modes and criteria and the need for new design concepts and analytical procedures. These can be provided only when all failure mechanisms that affect the performance of composite structures are identified and understood. In addition, experimental test programs must be conducted to substantiate design concepts, verify analytical procedures, and provide the data necessary to assure that composites can be safely applied to primary aircraft structures.

This report describes the design of a stiffened composite curved panel that satisfies the requirements for a pressurized passenger transport fuselage. The panel represents a minimum weight design, constrained by practical considerations and is based on current technology. Durability and damage tolerance requirements, similar to those governing the design of metallic fuselage structures were incorporated in the design.

A key point in justifying composites in fuselage construction is that of allowing the shell to go in the post-buckling range, as is done with metallic structures. Significant additional weight savings may be realized over buckling resistant design. Extensive testing of stiffened composite panels conducted at Lockheed has verified theoretical analyses and has demonstrated that composites can be safely loaded beyond the initial buckling limit for the load levels and skin gages considered in practical fuselage design. For this reason, post-buckled skin design was considered current technology for this program although several minor problems remain to be resolved.

STRUCTURAL REQUIREMENTS

A realistic set of structural requirements are defined below for the design of a representative stiffened composite curved fuselage panel. These

requirements provided the basic data for the design effort and encompassed:

1. A definition of the geometry requirements for the structure.
2. The development of a representative set of internal loads for design.
3. A definition of the material properties for the T300/5208 system.
4. The establishment of the design strain level and buckling criteria.

Basic Design Requirements

The final stiffened panel configuration is a minimum weight design, although practical constraints were imposed to assure safety, producibility and cost effectiveness. The panel is a skin/stringer design with internal frames and includes stiffener attachments and fail-safe considerations. The panel is 152.4 cm (60.0 inches) in length, 101.6 cm (40.0 inches) in width and has a constant radius of 298.5 cm (117.5 inches). Stiffnesses of frames and stringers are representative of those used on current transport fuselages. NARMCO T300/5208 graphite/epoxy has been used as the material system for this design.

Definition of Internal Loads

The internal loads used for the panel design study include ultimate loads specified by NASA and other types of loading that can reasonably be expected to occur on fuselage structure of commercial airplanes. The NASA requirement specified that the panel be capable of simultaneously carrying 0.525 MN/m (3000 lb/in) of ultimate longitudinal compression load and appropriate pressure conditions and 0.105 MN/m (600 lb/in) of shear load. The other conditions include (1) a longitudinal tension loading representative of a fuselage bending condition, (2) an ultimate ground test pressure condition, and (3) the appropriate loads for the damage tolerance (fail-safe) and fatigue requirements. The in-plane loads for these basic types of conditions are combined with their corresponding pressure loadings to form the complete internal loads environment for the design study.

Fuselage Pressurization Loads

The fuselage pressurization loads are based on the pressurization system designed for the baseline L-1011 airplane. This system provides a 2400 m (8000 ft) cabin altitude at 12,800 m (42,000 ft). The following control and relief valve pressures serve as the basis for defining the design pressures:

VALVE SETTING	PRESSURE	
	N/m^2	psi
Nominal Positive Differential Pressure (Control valve nominal setting)	0.0582	8.44
Upper Limit of Positive Relief Valve Setting	0.0609	8.835
Upper Limit of Negative Relief Valve Setting	-0.0034	-0.50

Based on these pressures the following fuselage pressurization loads were used when they add to the basic internal loads and ignored when they subtract. Aereodynamic pressure was not considered for this study.

CONDITION	PRESSURE, N/m^2 (psi)	
	POSITIVE	NEGATIVE
Ultimate Design Flight Conditions (1.5 times the upper limit setting)	0.0914 (13.25)	-0.00517 (-0.75)
Ultimate Ground Test Condition (1.33 x 1.5 times the upper limit positive setting)	0.1215 (17.63)	N.A.
Nominal Positive Differential Pressure	0.0582 (8.44)	N.A.

Internal Loads

After reviewing the design conditions of the forward fuselage for the L-1011 Commercial transport, a region was selected for which the ultimate design loads closely correspond to those specified by NASA. Additional critical load conditions were then established to provide the basis for the structural

analysis. These loads provided the means for evaluating the static, fatigue, fail-safe and ground test design requirements on the composite panel. Table 1 presents a summary of these conditions and their corresponding internal loads. The appropriate pressurization loads for these conditions are included to categorize the complete loads environment.

TABLE 1. INTERNAL LOADS FOR FORWARD FUSELAGE

CONDITION	INPLANE LOADS, MN/m (lb/in.)		PRESSURE, N/m^2 (psi)	
	AXIAL	SHEAR	MAX. POSITIVE	MAX. NEGATIVE
Ultimate Design				
o Compression - Shear	-0.525 (-3000)	0.105 (600)	0.0914 (13.25)	-0.00517 (-0.75)
o Tension - Shear	0.262 (1500)	0.105 (600)		
Ultimate Ground Test	-	-	0.1215 (17.63)	-
Damage Tolerance (Fail-Safe)				
o Residual Strength (2.5g Maneuver)	-0.350 (-2000) 0.175 (1000)	0.070 (400) 0.070 (400)	0.0582 (8.44)	-0.00344 (-0.50)
o Residual Strength (1.0g Flight)	-0.140 (- 800) 0.070 (400)	0.028 (160) 0.028 (160)	0.0640 (9.28)	-
Damage Tolerance (Discrete Source)				
o Residual Strength (Arbitrary 2.5g Maneuver)	-0.245 (-1400) 0.122 (700)	0.049 (280) 0.049 (280)	0.0640 (9.28)	-0.00379 (0.55)

Material Properties

The NARMCO T300/5208 graphite/epoxy material system was selected as the primary material for the design study. Both unidirectional lamina property data, and laminate design allowables compiled under the Advanced Composite Vertical Fin program (NASA/LaRC Contract NAS1-14000) were used to define the properties of the selected material.

Strains, elastic properties and physical constants for unidirectional lamina are presented in Table 2. These data represent room temperature dry (RTD), 82°C wet and -54°C dry conditions of T300/5208 graphite/epoxy material with a fiber volume between 62 to 67 percent.

TABLE 2. KEY UNIDIRECTIONAL PROPERTIES OF T300/5208 GRAPHITE/EPOXY

PROPERTIES		UNITS	RTD	82°C WET	-54°C DRY
Design Strains	Longitudinal Tensile Ultimate	10^{-3} m/m	9.00	9.00	9.00
	Transverse Tensile Ultimate	10^{-3} m/m	7.50	7.00	7.00
	Longitudinal Compression Ultimate	10^{-3} m/m	10.00	9.00	9.80
	Transverse Compression Ultimate	10^{-3} m/m	15.00	13.00	14.00
	Inplane Shear Ultimate	10^{-3} m/m	23.00	25.00	20.00
Elastic Properties	Longitudinal Tensile Modulus	GPa	137.90	139.97	134.45
	Transverse Tensile Modulus	GPa	11.03	9.65	12.27
	Longitudinal Compression Modulus	GPa	131.00	124.11	134.45
	Transverse Compression Modulus	GPa	10.76	9.38	12.07
	Inplane Shear Modulus	GPa	5.52	4.14	5.93
	Major Poisson's Ratio	-	0.27	0.26	0.28
Physical Constants	Fiber Volume	%	62-67	62-67	62-67
	Density	Mg/m^3	1.605	1.605	1.605
	Ply Thickness	mm	0.127	0.127	0.127
	Longitudinal Coefficient of Thermal Expansion	$\mu m/(m \cdot C)$	0.432	0.504	0.360
	Transverse Coefficient of Thermal Expansion	$\mu m/(m \cdot C)$	29.16	33.84	27.18

RTD = room temperature (dry)

Laminate preliminary design curves for the T300/5208 system are presented in Figures 1 through 7. These allowables are based on test data and are statistically based on 90 percent exceedance with a 95 percent confidence level. Notched and unnotched data are presented, with the notched allowables based on gross area stress with a 0.48 cm-diameter hole at a 2.54 cm spacing. The effects of temperature and moisture are included in these allowables so no additional factors should be included.

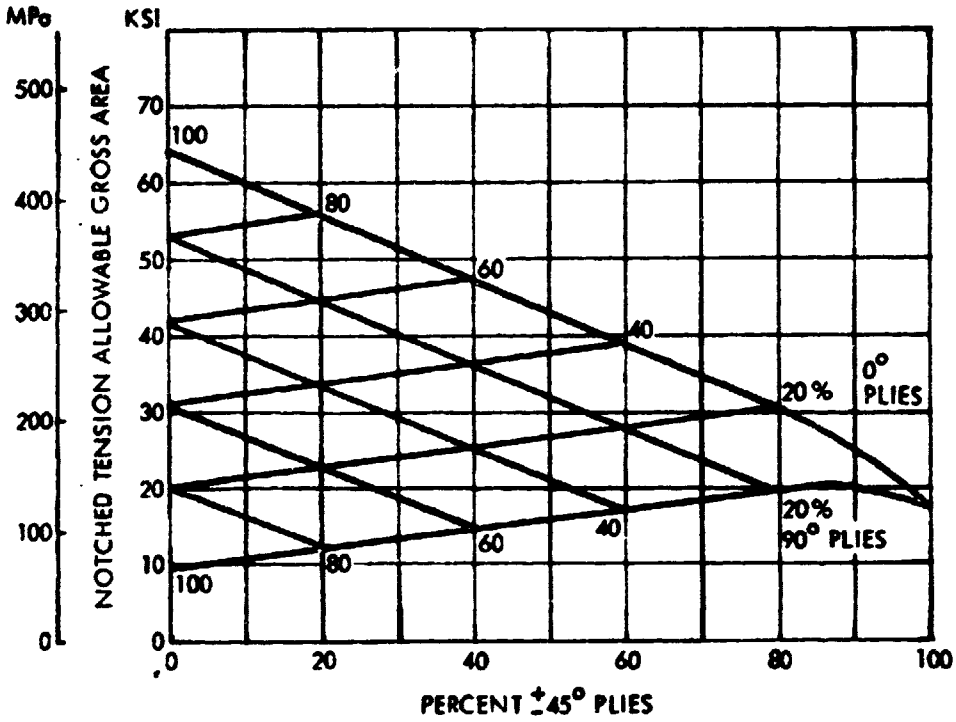

Figure 1. Notched Tension Allowables, T300/5208 Graphic/Epoxy

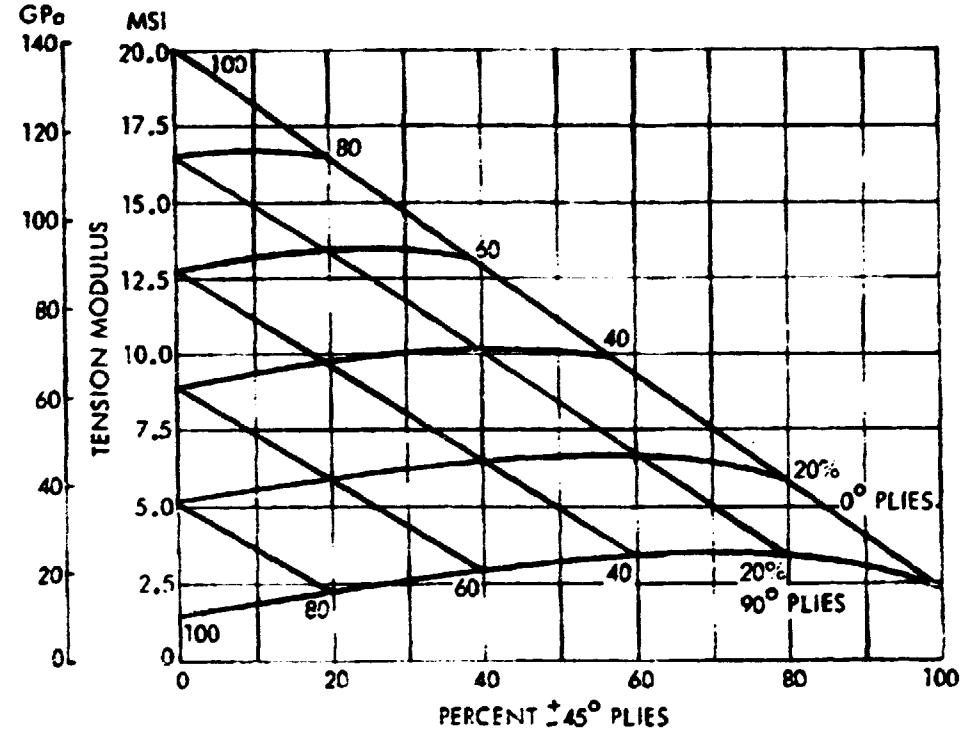

Figure 2. Tension Modulus of T300/5208 Graphite/Epoxy

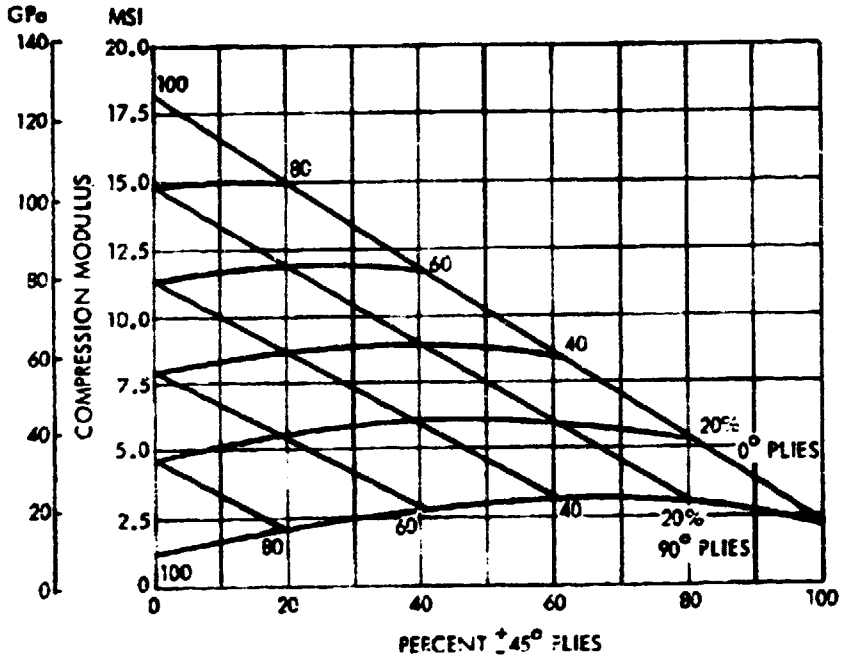

Figure 3. Compression Modulus of T300/5208 Graphite/Epoxy

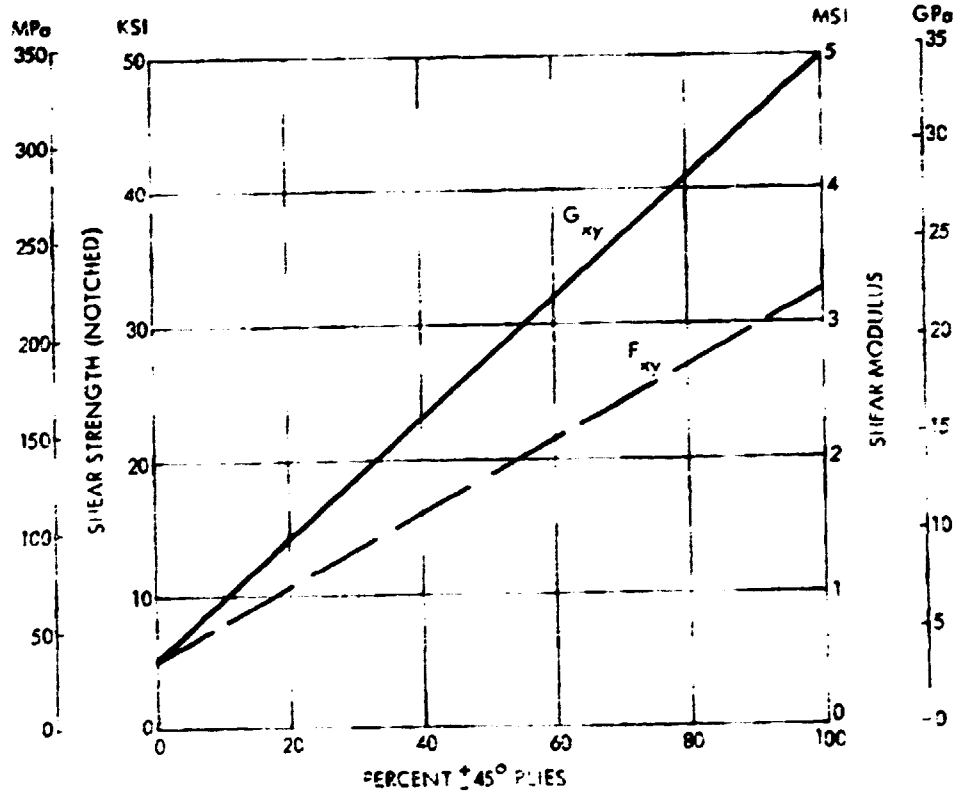

Figure 4. Notched Shear Strength and Modulus of T300/5208 Graphite/Epoxy

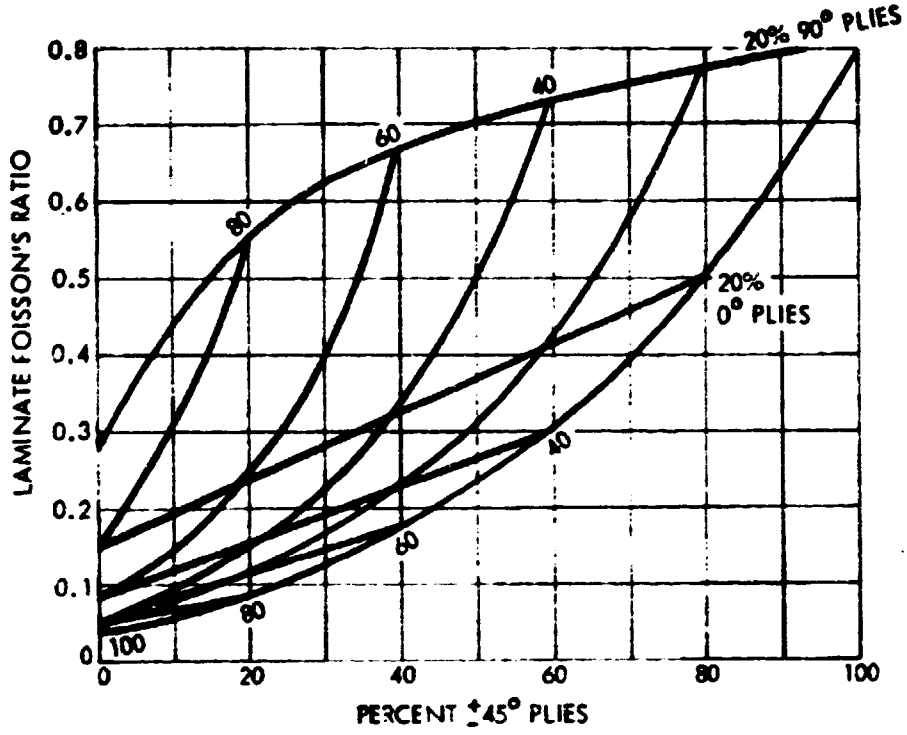

Figure 5. Poisson's Ratio of T300/5208 Graphite/Epoxy

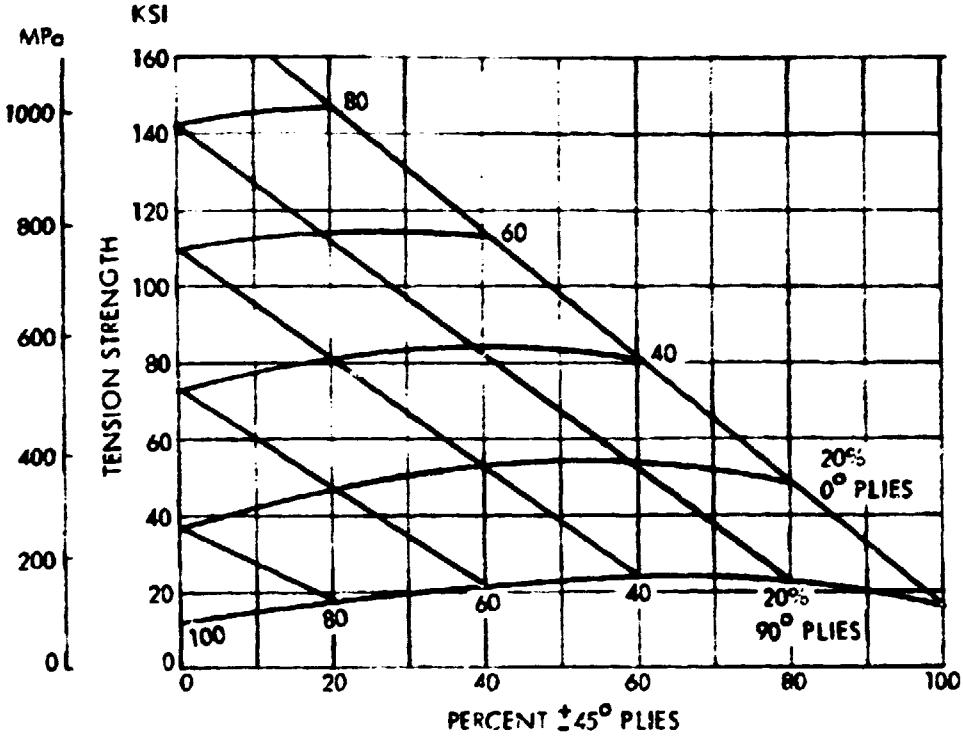

Figure 6. Tension Strength (Unnotched) of T300/5208 Graphite/Epoxy

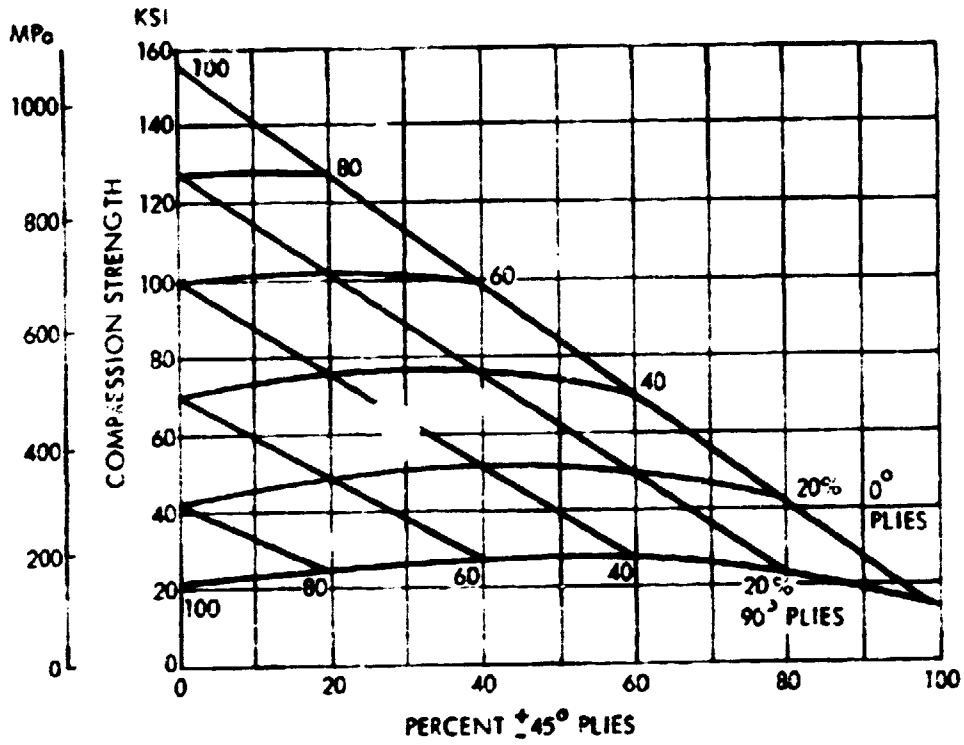

Figure 7. Compression Strength (Unnotched) of T300/5208 Graphite/Epoxy

Design Strain Levels

In the design of aluminum fuselage structure the damage tolerance (fatigue and fail-safe) requirements are generally achieved by limiting the permissible design stress/strain levels for static ultimate design conditions and certain operating conditions. These values are based on experimental data and related experience and successful service history of past aluminum transports. Since these historical design data do not exist for graphite/epoxy structure, conservative design strain levels must be established to cover the many considerations affecting the damage tolerance aspect of design.

Ultimate and working design strain levels were established for the T300/-5208 material system for the design study. These design strain levels were based on considerations including stress concentrations associated with cut-outs, joints and splices; by tolerance for impact damage; by transverse cracking in the 90-degree fiber-oriented plies; and by compatibility with adjacent aluminum strain levels. These considerations restricted the design ultimate

strains to approximately 50 percent of the composite material failure strain or a value of 4500 μ m/m and practical working strain levels to 3000 μ m/m. Table 3 presents the design strain levels used for this study. A more detailed description of the rationale used in arriving at these design strain levels is given in Reference 1.

TABLE 3. DESIGN STRAIN LEVELS

CONDITION	DESIGN STRAIN (μ in./in.)
Ultimate Design Flight	$\pm$4,500
Ultimate Ground Test	$\pm$4,500
Design Tolerance (Fail-Safe)	
o Residual Strength	$\pm$3,000
Damage Tolerance (Discrete Source)	
o Residual Strength	Not Applicable

NOTES:

1. Restrict the maximum ply level unidirectional strain to the specified values.

Buckling Limitations

In the design of commercial aircraft, restrictions are placed on the post-buckling behavior of the fuselage shell to ensure adequate fatigue life during operation. These restrictions are generally applied to the initial buckling strength of the skin between stringers or longerons.

Current wide-bodied aircraft o the L-1011 type generally require that the pressurized structure be unbuckled under 1 g level flight loads in combination with normal pressure loads. In addition to this requirement, the L-1011 fuselage skins are designed such that the ultimate design shear flows do not exceed five times the initial shear buckling value, i.e. $q_{ult}/q_{cr} \leq 5$. In actual design, however, shear flows will rarely exceed three times the critical value.

Recent fatigue tests under cyclic shear loading conducted at Lockheed indicate fatigue failures are not likely to occur in the range of 10^4 to 10^5 cycles in J-stiffened composite panels if the ratio of ultimate shear to critical shear is in the order of 3:1. This requirement and the requirement for unbuckled skin at 1 g level flight appear to be realistic constraints for the design of composite fuselage structure and were used as criteria for the design study.

The post-buckling behavior of the skin in compression will generally be controlled by instability of the stiffeners or by maximum strain limitations and no additional restrictions need to be imposed on the design.

SKIN-STRINGER PANEL SIZING

Stiffener Concept Selection

Discrete open-section stiffeners such as I, J, Z and blade stiffeners have been the most popular concepts used in metallic fuselage design and, along with hat-stiffened panels, were selected for evaluation in the composite panel design. The primary considerations were structural efficiency, producibility and cost. Hat-stiffened panels were found to have a higher structural efficiency than panels with open-section stiffeners and are clearly the preferred concept for highly loaded wing panels and areas where skin buckling is not permitted. In fuselage panels, the relatively low load intensities coupled with producibility and cost advantages, however, make open sections more attractive. In addition, attachment of substructure and equipment, and provisions for joints and splices, are more easily accomplished for open-section stiffeners.

Z-section stiffeners were eliminated from consideration because of the poor pull-off capability provided by the single skin attach flange in cocured or adhesively bonded construction. I and J stiffeners were found to have a slight edge in structural efficiency over blade stiffeners, especially in the presence of eccentricities, but all three configurations were considered throughout the preliminary design process. The J-section configuration was selected for the final design as offering the best compromise when considering structural efficiency and ease of manufacturing.

Method of Analysis - Buckled Skin Design

A preliminary design procedure, LG-062-OPT, developed at the Lockheed-Georgia Company has been used in sizing the post-buckled skin design. The procedure consists of a series of closed form analysis routines which are coupled with the COPES/CONMIN program to provide an efficient panel sizing code. COPES/CONMIN is a nonlinear mathematical programming optimizer for the minimization of functions with inequality constraints and was written by Vanderplaats (Reference 2). Details of the analyses and assumptions used therein are briefly described in the following sections. Data and illustrations presented refer to the final panel design, unless otherwise noted.

Load Distribution

The total panel loading is defined by the inplane stress resultants, N_x, N_y, N_{xy}, and the moment M_x due to initial eccentricities, where x is the longitudinal coordinate. The moment is a function of N_x and causes a curvature, K, in the x-z plane. In the present analysis, the stress resultants N_y and N_{xy} are taken entirely by the skin, while the longitudinal loading is carried jointly by the skin and stringers, or

$$N_x = N_1 + N_{xst} \qquad N_y = N_2 \qquad N_{xy} = N_{12}$$

where N_1, N_2 and N_{12} are the average stress resultants in the skin. The stringer loading can be expressed in terms of the panel edge strain ϵ_1 and the curvature K

$$N_{xst} = \frac{EA_{st}}{b_s} \left(\epsilon_1 - \bar{z}_{st} K\right) - N^T_{xst}$$

where EA_{st} is the extensional stiffness of the stringer, b_s is the stringer spacing, $\bar{z}_{st}$ is the distance from the skin center line to the stringer centroid and N^T_{xst} is the equivalent thermal load. Since the load/strain response of the skin in the post-buckling range is nonlinear, an iterative procedure is used to determine the distribution of loading between skin and stiffeners. Reduced tangent and secant moduli are calculated at each step. When the panel is loaded beyond the initial buckling limit of the skin, the portion of the longitudinal load carried by the stringers increases as the

total load, N_x is increased. This is illustrated in Figures 8 and 9 for different loading conditions. The effect of pressurization on the stringer loading is shown in Figure 8. A hoop tension of 0.273 MN/m corresponds to a maximum positive pressure of 0.0914 N/m^2 (13.25 psi) and a hoop compression load of 0.0158 MN/m represents a maximum negative pressure of 0.00517 N/m^2

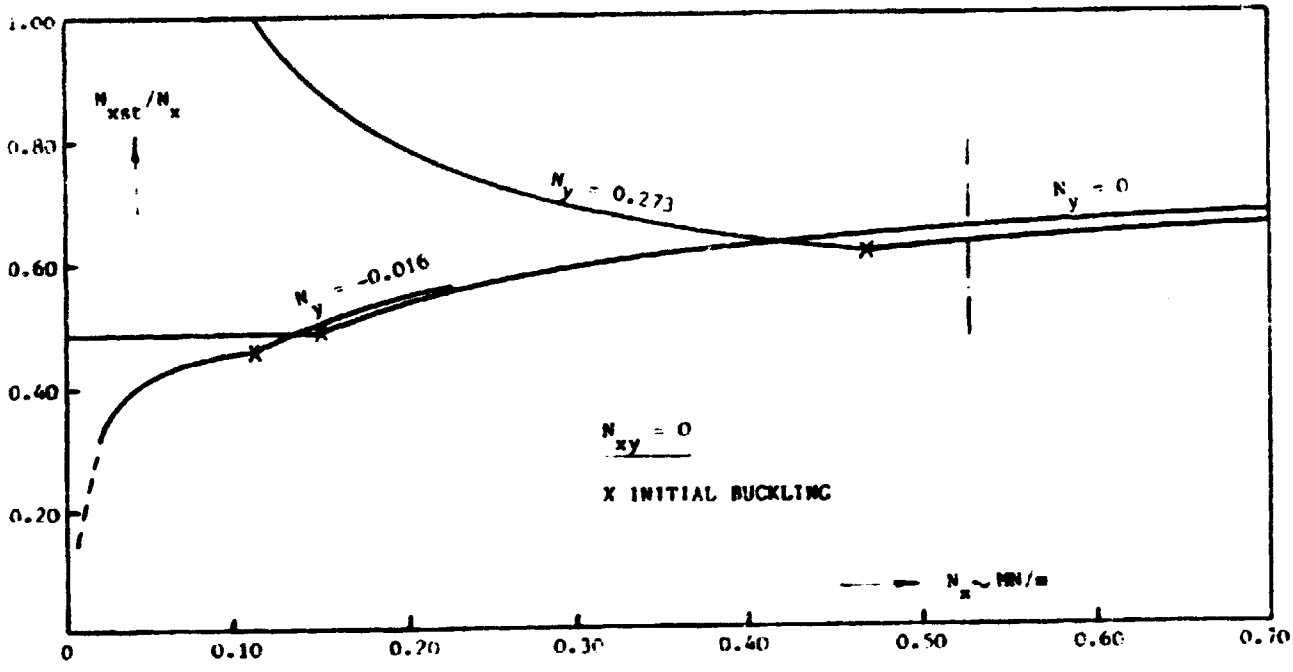

Figure 8. Stiffener Load-Effect of Pressurization

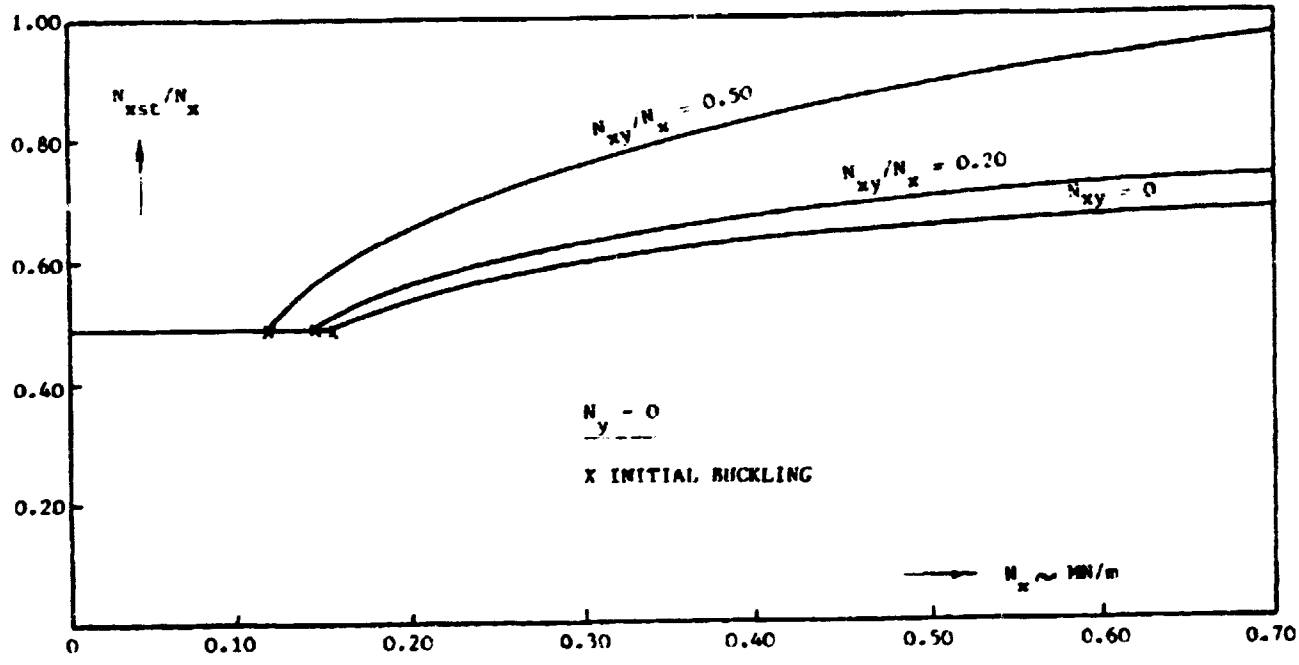

Figure 9. Stiffener Load-Effect of Inplane Shear

(0.75 psi). It is seen that the initial buckling load is increased significantly in the presence of hoop tension and decreased by hoop compression but that at the design load of 0.525 MN/m (3000 lb/in.), there is only a few percent change in stiffener load as a result of pressurization. As shown in Figure 9, the presence of in-plane shear reduces the initial buckling limit of the skin and therefore increases the share of the total longitudinal load reacted by the stringers. A shear load of 0.105 MN/m (600 lb/in.) causes an increase of 7 percent in the stringer load at the design condition of 0.525 MN/m compression.

Initial Eccentricities

To account for manufacturing tolerances, laminate thickness variations and other imperfections, initial bow-type eccentricities are considered in the analysis. The eccentricities are assumed to vary sinusoidally along the length L of the panel and have amplitude e. Values of e/L ranging from 0.001 to 0.002 are normally used in the design of compression panels. In the present analysis e/L = 0.001 was assumed. Curvatures are calculated using a beam column approach and the resulting strains are added to those produced by in-plane loading. These calculations involve the determination of the Euler wide column load of the skin-stringer combination

$$N_{EULER} = \frac{\pi^2 EI_T}{b_s L^2}$$

The tangent stiffness EI_T is defined as the slope of the M_x/K curve and is therefore a function of the applied load N_x. As a result, the Euler load drops sharply at initial buckling and continues to decrease in the post-buckling range. This sharp drop in load is shown in Figure 10.

Average Stress Resultants in Buckled Skin

This analysis predicts the behavior of anisotropic plates loaded in the post-buckling range by a combination of in-plane biaxial compression, or tension, and shear. The shear field theory, originally developed by Koiter

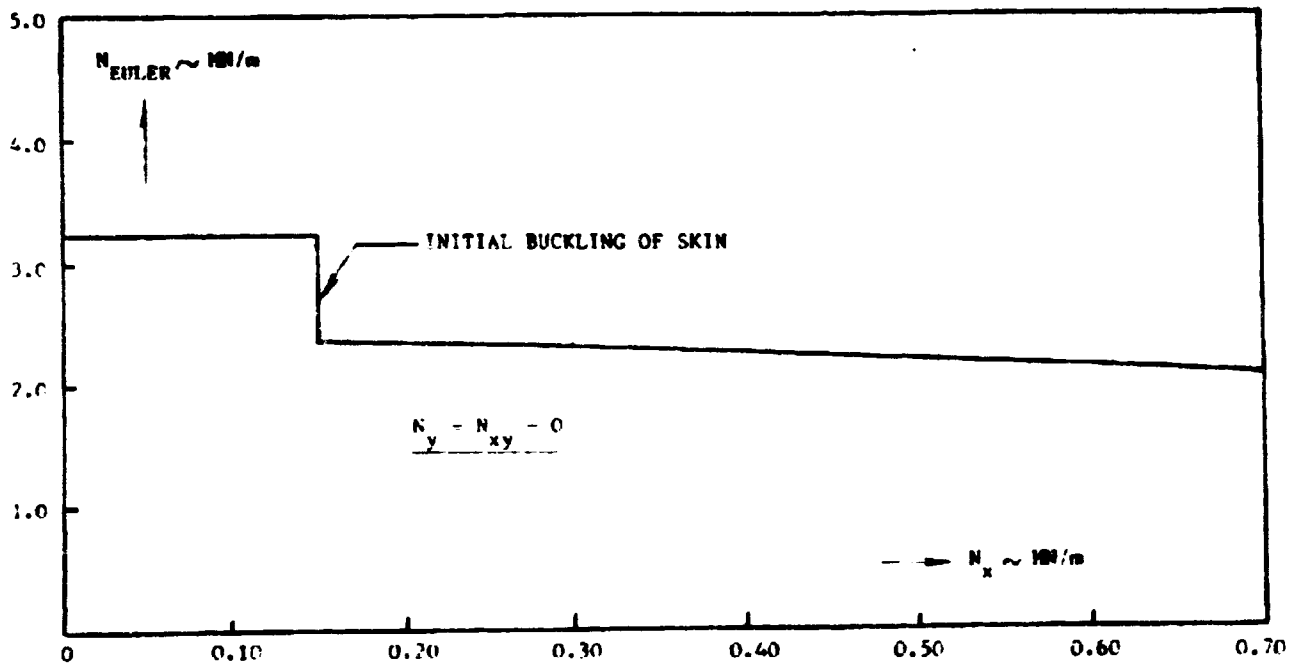

Figure 10. Euler Load in Post-Buckling Range

(Reference 3) for long isotropic plates, was extended to include the case of symmetrically laminated composite plates. The buckling displacement pattern used in the analysis is expressed by

$$w(x, y) = W(y) \sin \frac{\pi}{\lambda} (x - my)$$

in which λ is the half wave length of the buckle in the longitudinal (x) direction and m defines the inclination of the nodal lines in the presence of shear. To extend the validity of the analysis into the advanced post-buckling regime, the function W(y) is taken as a constant (W = f) in a center strip of width equal to $(1 - \alpha)\, b_s$. Nodal lines are assumed along the stiffeners and hence in the edge zones, $0 \leq y \leq 1/2\, \alpha\, b_s$, the function W(y) is taken as

$$W(y) = f \sin \frac{\pi y}{\alpha b_s}$$

The Rayleigh-Ritz energy method is used to determine the four unknown wave parameters, λ, m, f and α.

Relations may be established between the average stress resultants in the skin (N_1, N_2, N_{12}) and the strains at the plate edges ($\epsilon_1, \epsilon_2, \gamma_{12}$). These relations are shown for the final skin lay-up of the stiffened panel design, a 16-ply $[90/\mp45/0_2/\mp45/0]_S$ laminate, in Figures 11, 12 and 13 for the cases of zero hoop tension, maximum hoop tension and maximum hoop compression, respectively. The stress resultants are normalized by N_{CR}, the initial buckling load in pure compression, and plotted as a function of the panel edge strain ϵ_1. The latter is normalized by ϵ^*, which represents the strain corresponding to N_{CR}. The values of N_{CR} and ϵ^* for the laminate under consideration are:

$$N_{cr} = .0770 \text{ MN/m } (440 \text{ lb/in})$$
$$\epsilon^* = .000578 \text{ m/m}$$

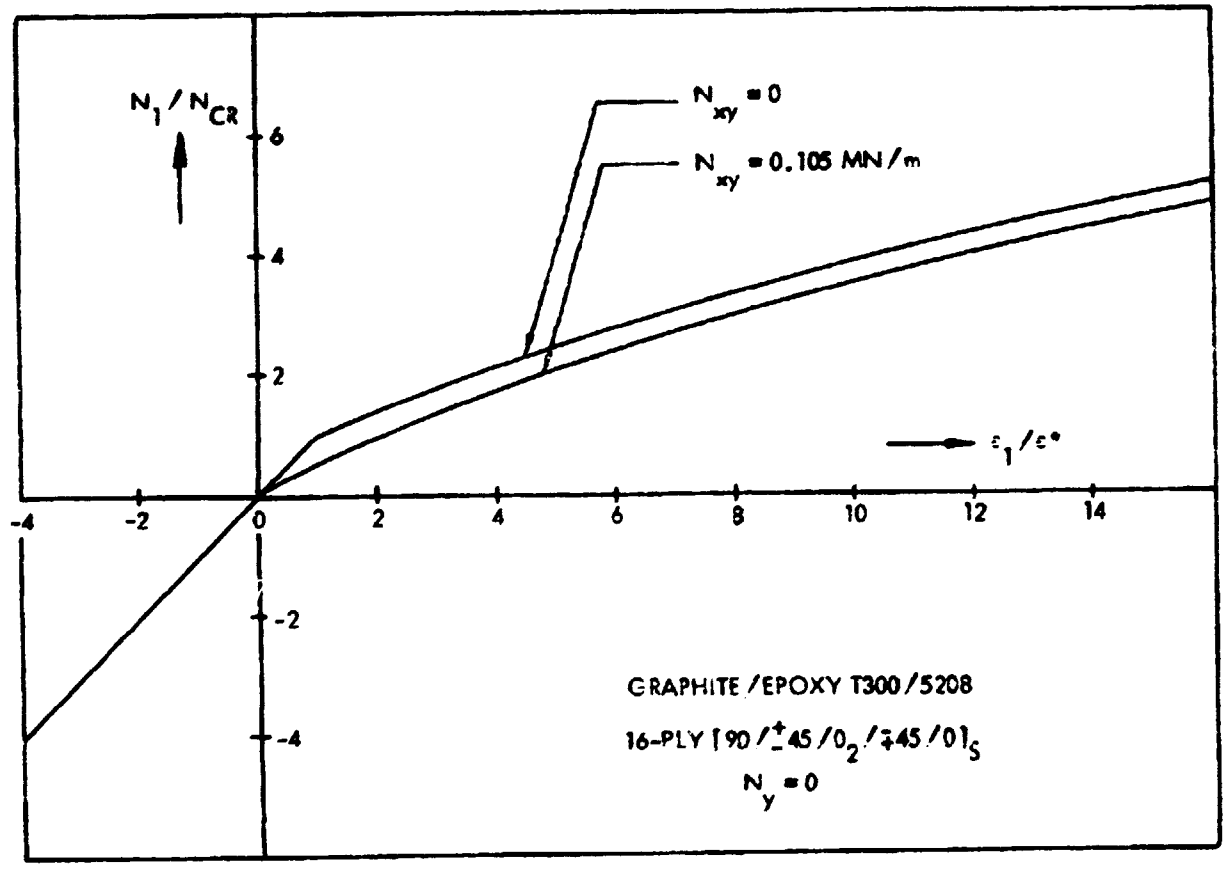

Figure 11. Stress-Strain Relations, Buckled Skin

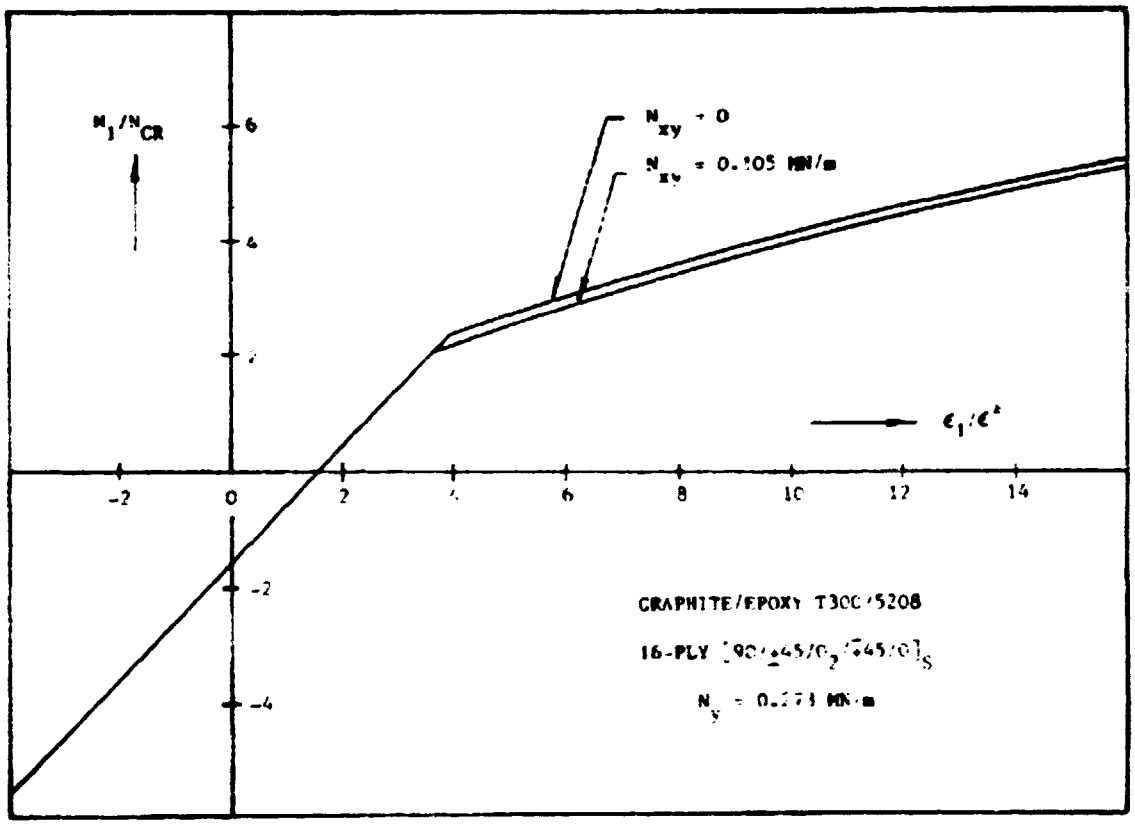

Figure 12. Stress-Strain Relations, Buckled Plate

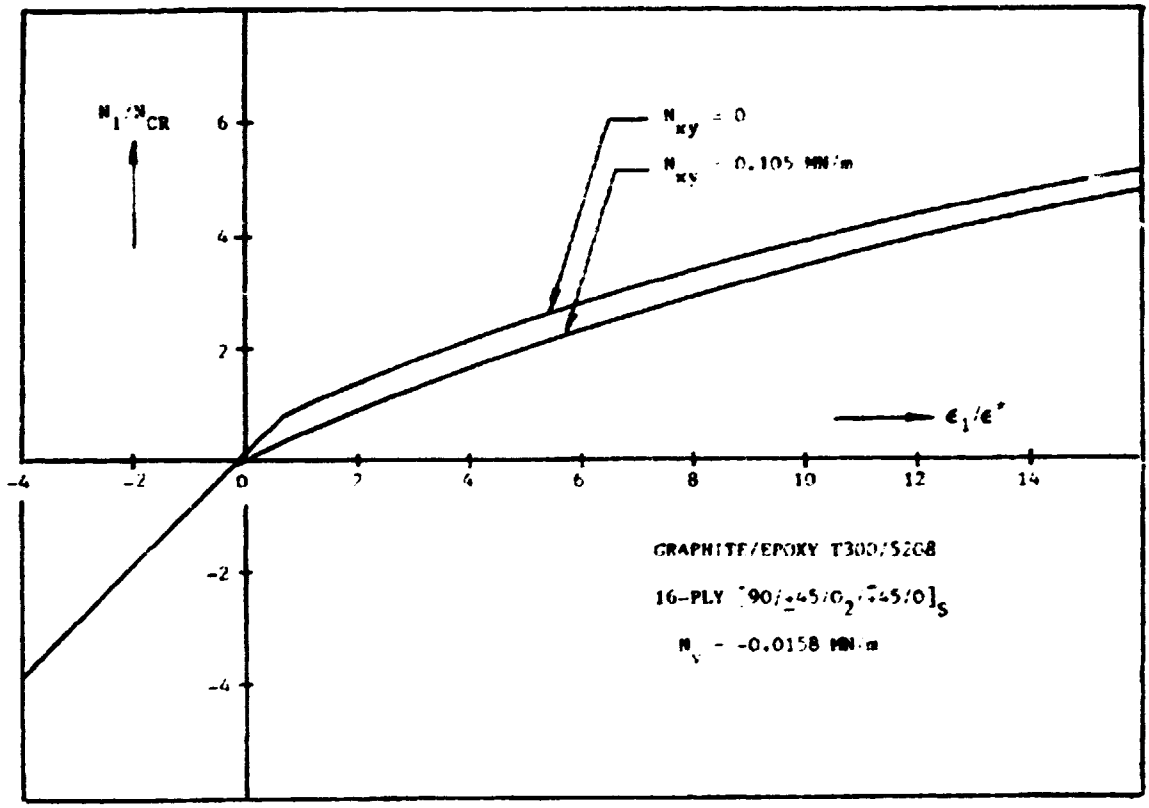

Figure 13. Stress-Strain Relations, Buckled Plate

Strains in Buckled Skin

As one of the failure modes considered in the program, strains in the skin are compared with material allowables or specified strain limits. Figure 14 shows the strains in the 16-ply final skin laminate, when the latter is loaded in pure compression. The maximum membrane strain occurs along the plate edges

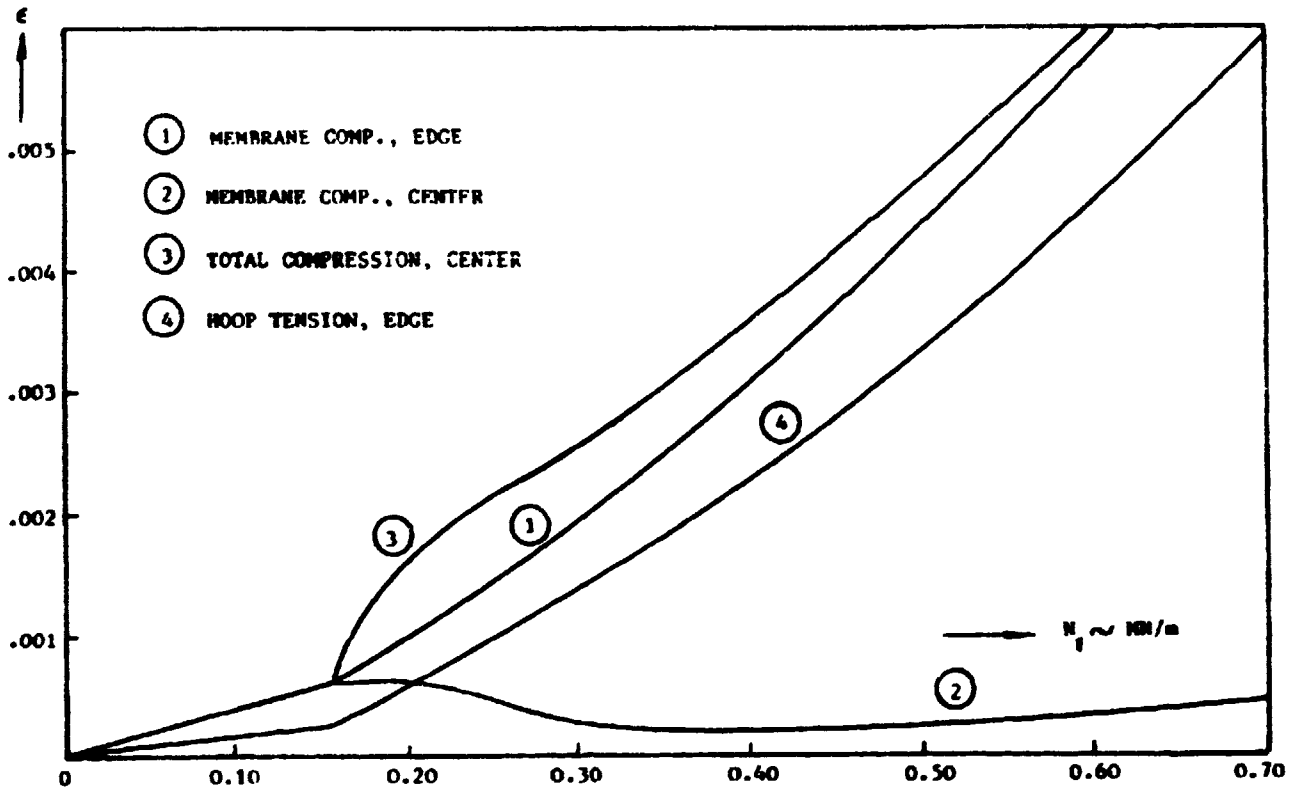

Figure 14. Strains in Buckled Skin

and is plotted in Figure 14 as a function of the average stress resultant, N_1, in curve ① . The membrane strain in the center of the plate, curve ② , changes little from its initial buckling value and even drops slightly. Large bending strains exist in the center of the plate, however, and the total compressive strain generally exceeds the edge strain, as shown by curve ③ . The hoop tensile strain developed in the skin, when subjected to longitudinal compression only, is shown by curve ④ . In computing margins of safety, the plate edge strain ① and the hoop tension strain ④ are compared with the imposed strain limit of 0.0045, whereas the margin for the total strain ③ will be based on ply level material allowables (Table 2).

Buckled Plate Stiffnesses

To account for the effect of the attached post-buckled skin in stringer instability analyses, the stiffnesses of the skin with respect to incremental deformations must be determined. The coefficients of the reduced (tangent) stiffness matrix are given by

$$A^{*}_{ij} = \frac{\delta N_i}{\delta \epsilon_j} \qquad i, j = 1, 2, 6$$

in which N_1, N_2 and $N_6 = N_{12}$ are the average stress resultants and ϵ_1, ϵ_2 and $\epsilon_6 = \gamma_{12}$ are the strains at the plate edges.

To illustrate the magnitude of these stiffnesses, the ratios A^{*}_{11}/A_{11}, A^{*}_{22}/A_{22} and A^{*}_{66}/A_{66} are plotted in Figure 15 as a function of the longitudinal strain ratio ϵ_1/ϵ^{*} for the final skin laminate, when the latter is loaded in pure compression. The A_{ij} represent the stiffness coefficients for the unbuckled plate.

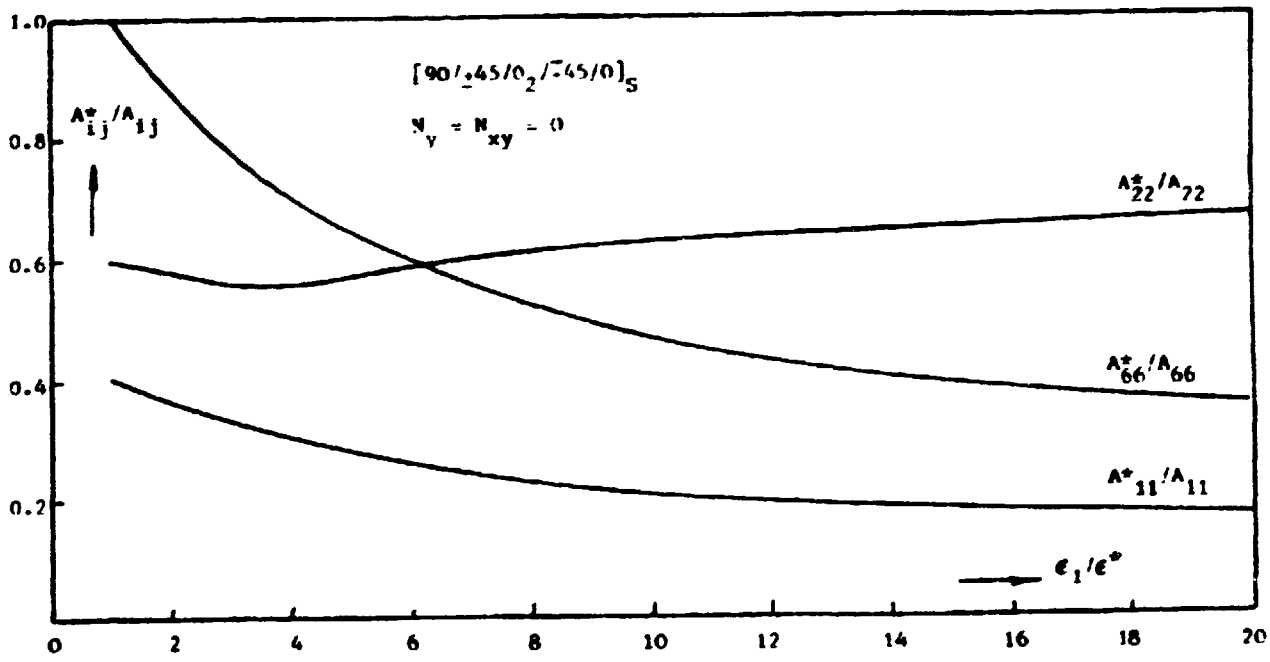

Figure 15. Reduced Stiffnesses, Post-Buckled Plate

Buckling of Stiffeners

In panels with buckled skin, instability of the stringers becomes an especially important failure mode. Stringers of thin-walled open cross section, generally buckle in a torsional or torsional-flexural mode. A torsional-flexural buckling analysis (TCFLX) was developed and incorporated as a subroutine in the present panel sizing code. In this analysis, an arbitrary number (N) of uniformly spaced stringers is allowed to participate in the buckling process. The effect of the attached skin is accounted for by replacing the skin by a set of equivalent forces. In the current version of TCFLX, the stringers are assumed to displace and rotate rigidly with respect to their shear center, i.e. cross-sectional deformation of the stiffener elements is neglected. The stiffener buckling load is obtained by solution of a 4Nx4N eigenvalue problem.

Design Optimization Results

The inplane load combinations considered in the minimum weight analyses of the skin-stringer design are shown in Table 4.

TABLE 4. IN-PLANE LOAD CONDITIONS

LOAD CONDITION	INPLANE LOADS, MN/m		
	N_x	N_y	N_{xy}
1	-0.525	0.273	0.105
2	-0.525	-0.0158	0.105
3	0.262	0.273	0.105
4	0.262	-0.0158	0.105
5	0	0.362	0
6	-0.525	0	0.105

Unbuckled Skin Design

The NASA-developed PASCO (Panel Analysis and Sizing Code) program (Reference 4) was used to perform the initial sizing of the unbuckled skin design. Load condition number 6 of Table 4 was selected to evaluate the relative structural efficiencies of I, J and blade stiffened panels.

The PASCO model for the I-stiffened panel configuration is shown in Figure 16. It consists of six repeating elements (stringer bays). Each repeating element is composed of fifteen plate elements in four different wall configurations: skin, stringer attachment flange, stringer web and free flange.

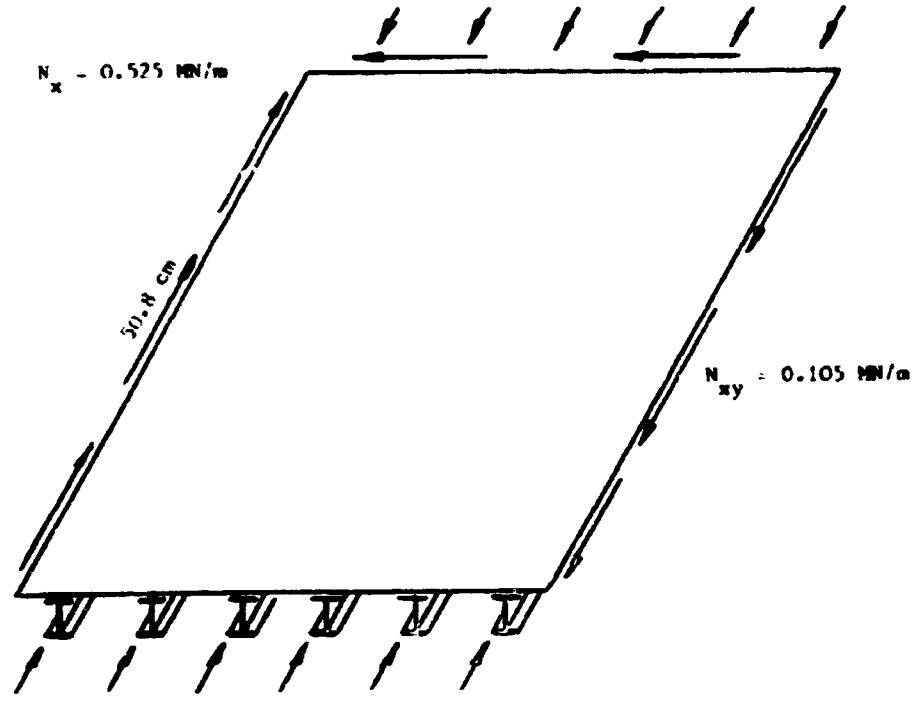

PANEL WITH DESIGN LOADING

(a) PASCO PANEL MODEL

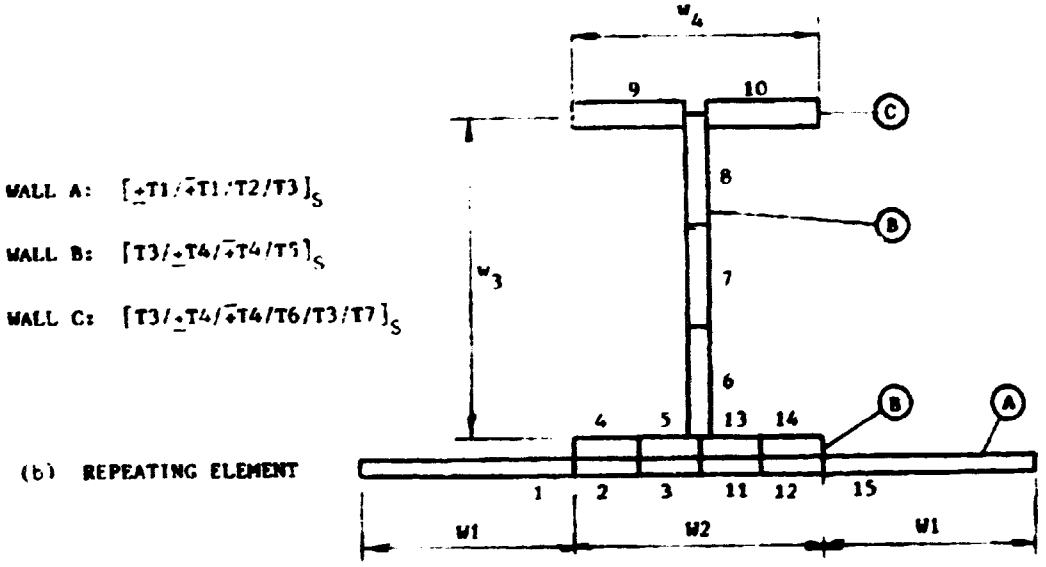

(b) REPEATING ELEMENT

Figure 16. PASCO Model

Lamina orientations for each wall configuration were limited to 0, 90 and ±45 degrees. The panel is 50.8 cm (20.0 inches) long and has its lateral edges simply supported. The maximum permissible strain in the panel was set at 0.0045. Results of the analysis for the I-stiffened panel are shown in Table 5.

The structural efficiencies of the three stiffener configurations analyzed are shown in Table 6. The I- and J-stiffened panels have approximately the same mass index but the blade stiffeners are considerably heavier. No attempts were made in these initial analyses to maintain practical constraints on stiffener dimensions and spacing, as is evident from the results in Tables 5 and 6. They did, however, establish a lower limit on the attainable minimum weight for buckling resistant panels at the required load level.

TABLE 5. PASCO ANALYSIS RESULTS, I-STIFFENED PANEL

LAYER	ORIENTATION DEG.	THICKNESS cm	ELEMENT	WIDTH cm
T1	45	0.0082	W1	1.90
T2	0	0.0295	W2	0.64
T3	90	0.0052	W3	2.62
T4	45	0.0052	W4	1.26
T5	0	0.0104		
T6	0	0.0468		
T7	0	0.0092		

TABLE 6. STRUCTURAL EFFICIENCY - BUCKLING RESISTANT PANELS

STIFFENER CONFIGURATION	PANEL WIDTH B, cm	MASS W, kg	MASS INDEX $W/ B L^2$ kg/m^3
I	26.61	0.5290	7.703
J	25.91	0.5303	7.931
Blade	42.21	1.0728	9.85

Buckling Resistant vs Post-Buckled Panels

To illustrate the weight reduction which can be realized by utilizing post-buckled panel design, optimum buckling resistant and post-buckled I-stiffened panels subject to load condition number 6 were obtained. The results are shown in Figure 17 in terms of panel mass index (weight/plan area/length) versus the ratio of stringer spacing to panel length, b_s/L. The post-buckled panel designs were obtained with LG-062-OPT. In order to compare the Lockheed sizing code with the NASA-developed PASCO program, unbuckled skin designs were also obtained with a version of LG-062-OPT in which skin buckling is considered a failure mode. In the latter, the skin is conservatively assumed to be simply supported at the stringers and the resulting weights are thus somewhat higher than those obtained by using PASCO.

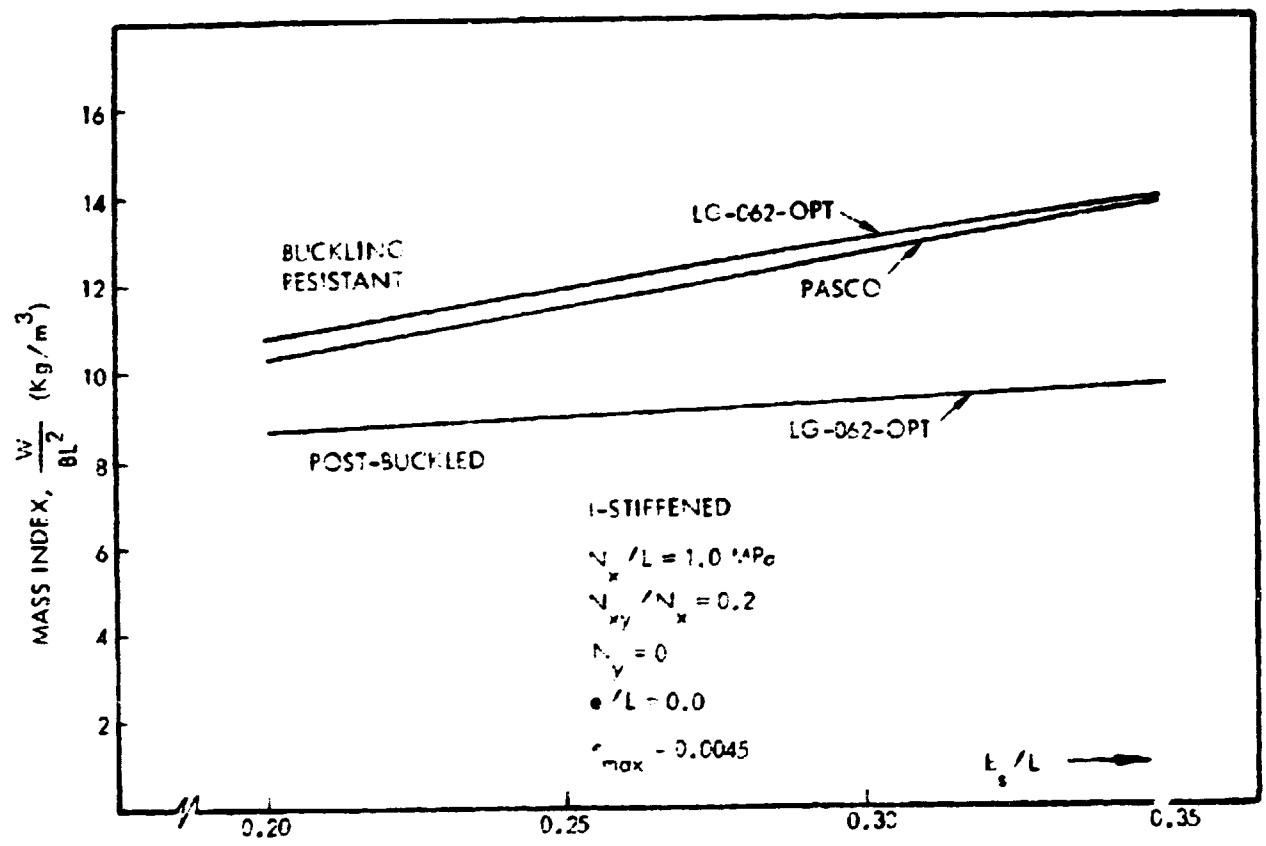

Figure 17. Buckled vs Unbuckled Panel Design

The range of stiffener spacings considered for this comparison is from 10.16 cm (4.0 inches) to 17.78 cm (7.0 inches). The geometry and construction of the stiffeners are shown in Figure 18. The post-buckled panel designs required w_{af} to be equal to w_f. The panels are assumed to have no initial bow. The longitudinal and transverse (membrane) strains for these analyses were limited to 0.0045.

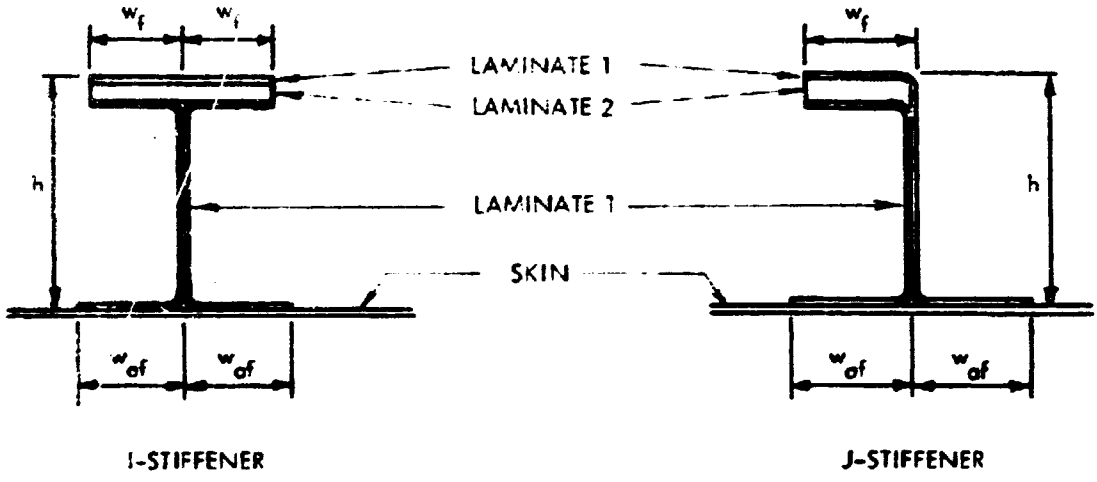

Figure 18. Stringer Geometry and Construction

Weight reductions of from 15 to 30 percent are possible for this case. An additional benefit of post-buckled design is the small weight penalty associated with an increase in stringer spacing when compared to that incurred in buckling resistant design. For example, when b_s/L is increased from 0.20 to 0.35, the buckling resistant panel weight is increased by 34 percent whereas the post-buckled panel weight is increased by only 11 percent. Thus, the stringer spacing in post-buckled panels may be determined by practical considerations such as fabrication cost, noise transmission or by structural considerations such as damage tolerance or skin pillowing.

An example of equivalent buckling resistant and post-buckled designs is shown in Figure 19. The buckling resistant design was determined by PASCO. The loading, geometry and strain limitations correspond to those used in obtaining the results in Figure 17.

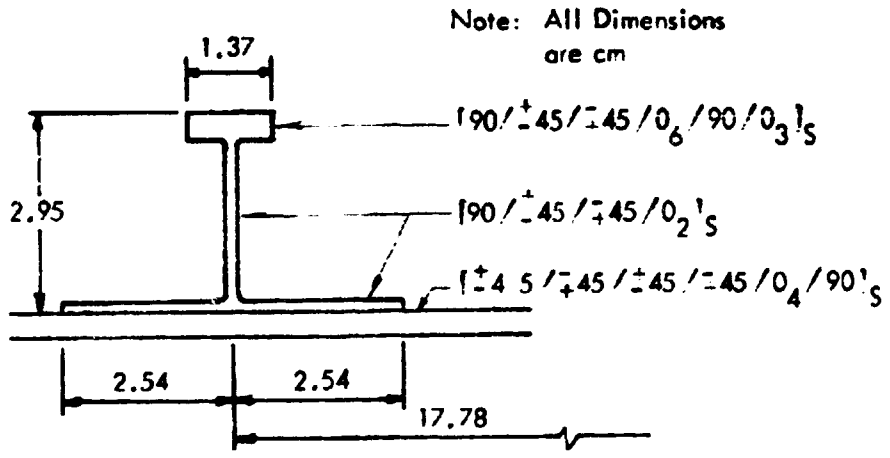

(a) BUCKLE RESISTANT DESIGN

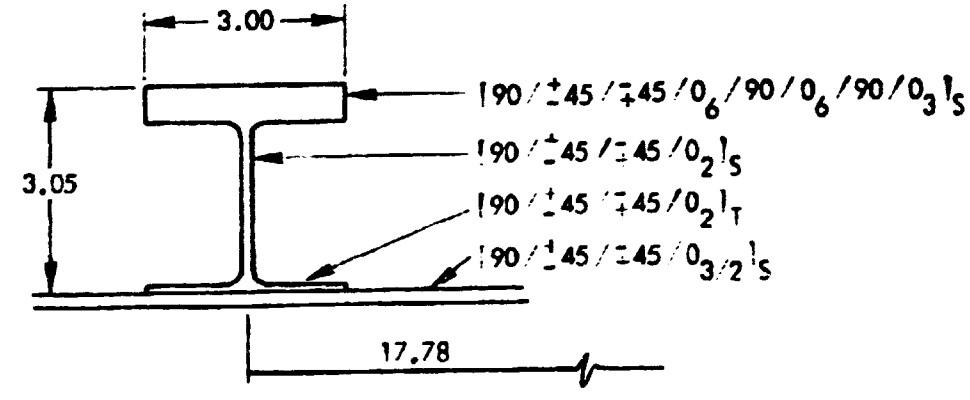

(b) POST-BUCKLED DESIGN

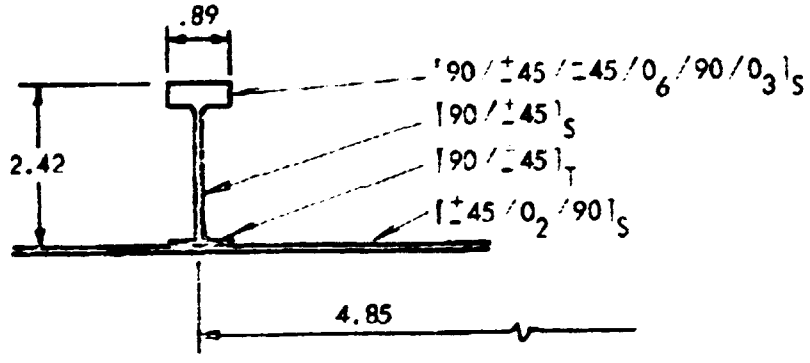

(c) ABSOLUTE OPTIMUM POST-BUCKLED DESIGN

Figure 19. Equivalent Panel Designs

As would be expected, the most striking variants between the two designs are the number of plies in the skin and the amount of material in the free flange. Once skin buckling is removed as a failure mode, material may be shifted from the skin to the stiffener where it is more efficiently used. In post-buckled design the skin lay-up may in large part be dictated by the ground test pressure condition (condition number 5, Table 4), fuselage torsional stiffness, damage tolerance, or by fatigue and acoustic requirements. In the post-buckled designs in Figure 17, the skin was required to have at least two 90-degree, eight 45-degree, and two 0-degree plies. Similarly, the stiffener web was required to have at least two 90-degree and eight 45-degree plies with 0-degree plies optional. The free flange was required to have sufficient 90-degree plies so that no more than six 0-degree plies are directly adjacent. These practical limitations on the minimum skin and stringer lay-ups constrain the panel to a nonoptimum but realistic design.

To show the effect of these limitations, an optimum post-buckled panel subject only to the last constraint was obtained with the stringer spacing set at 10.16 cm (4.0 inches). The mass index of this panel is 8.33 kg/m^3. This represents a four percent decrease from the corresponding (b_s/L = 0.2) design in Figure 17. If the stringer spacing is allowed to assume its optimum value, the mass index is further reduced to 7.18 kg/m^3. This absolute optimum design is shown in Figure 19c. The penalty associated with requiring a reasonable minimum number of plies and stringer spacing can be determined by comparing this last mass index with those in Figure 17. The penalty ranges from 21 percent to 34 percent for this case. For higher load levels, the optimum stringer spacing tends to increase as does the required number of plies to satisfy strength and stability requirements. Thus, the practical optimum design for higher load levels will likely be closer to the absolute optimum design, and the weight penalty will be reduced from that shown above.

When comparing post-buckled panel weights to buckling resistant panel weights, it is important to impose similar practical limitations on the designs. This was done in obtaining the results shown in Figure 17. The buckling resistant panel weights shown in References 5 and 6 must be compared to absolute optimum post-buckled designs. For example, Figure 6 of Reference 5 shows a mass index of 8.4 kg/m^3 for the loading presently considered. Here

the index has been factored up by the ratio of the density used in this study to that used in Reference 5. Comparing absolute optimum designs shows a 15 percent weight reduction for the post-buckled over the buckling resistant design. This is the same percentage difference between the practical optimum post-buckled and buckling resistant weights shown in Figure 17 for the smallest practical stringer spacing considered.

Effects of Load and Design Parameters on Panel Weight

The effects of loading combinations, initial imperfections, strain limitation and cross-sectional shape on post-buckled panel weight were studied under Lockheed IRAD and are reproduced here. These panel weights closely approach absolute optimum values since few practical limitations were placed on the number of plies in the skin or stiffeners or on the cross-sectional geometry. Although the weights should not be compared to those of practical fuselage panels, the trends of the effects of the various parameters on realistic panels should be similar to those shown in the results below.

Shear Loading - When no restrictins other than those of strength and post-buckled stability are placed on the panel design, the effect of shear loading on panel weight is substantial. Figure 20 shows this effect for panels with a stringer spacing to panel length ratio, b_s/L, of 0.25. Except at the lowest compression loading magnitude considered, weight penalties of 20 and 30 percent are associated with shear load ratios, N_{xy}/N_x, of 0.2 and 0.4, respectively.

Figure 21 shows the effect of shear and stringer spacing on panel weight for an intermediate compression load index, N_x/L = 1.0 MPa. The weight penalty due to shear increases as stiffener spacing is increased. Also shown in this figure are similar weights for buckling resistant panels. The penalty due to shear is relatively greater for post-buckled panels than for unbuckled panels. However, had a minimum number of 45-degree plies in the skin been imposed on the post-buckled designs, due for example to required shear stiffness, the weight penalties due to shear would have been considerably reduced.

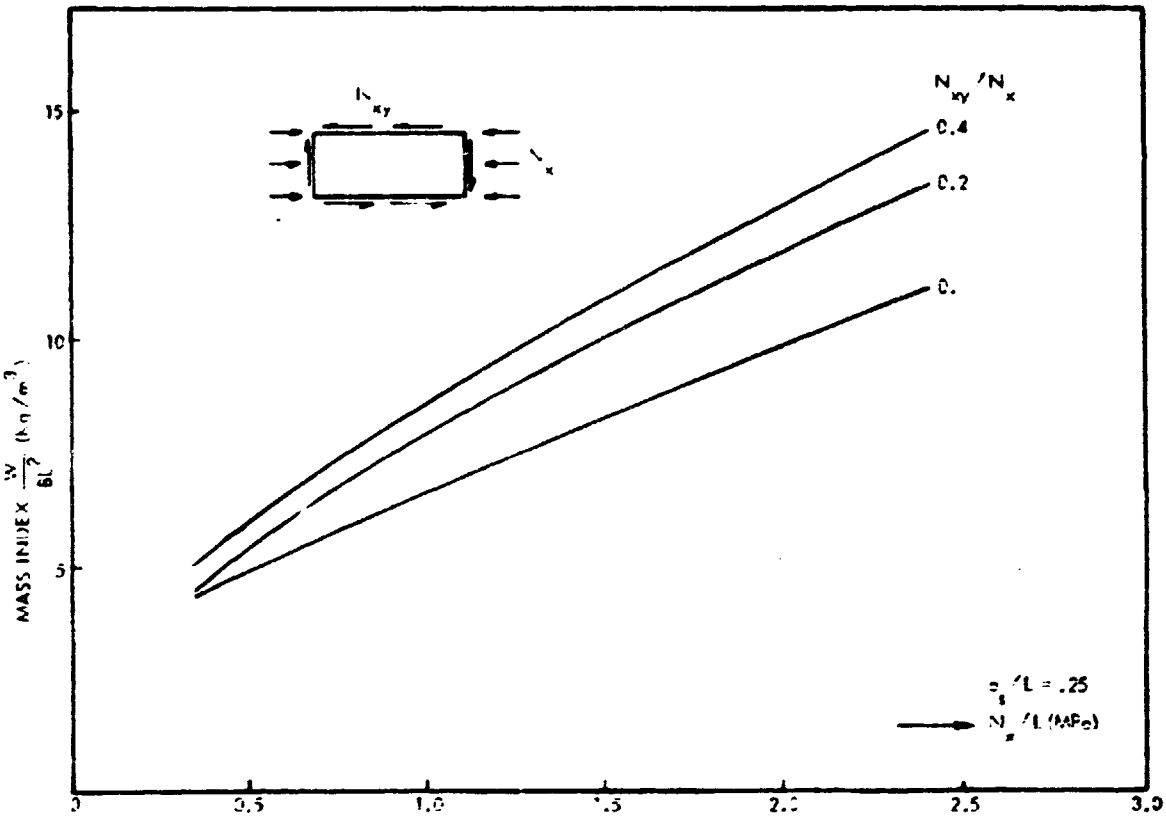

Figure 20. Effect of Shear on Panel Weight

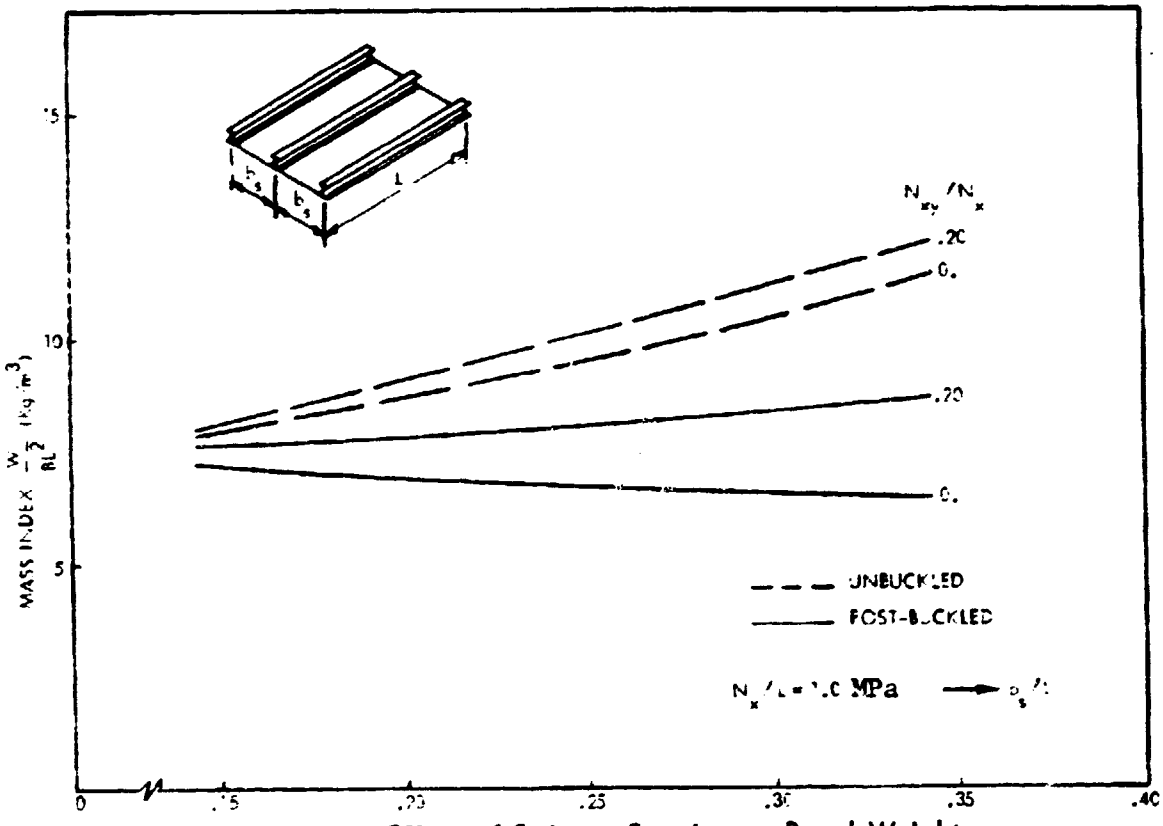

Figure 21. Effect of Stringer Spacing on Panel Weight

Another point of interest shown in Figure 21 is that when the shear to compression load ratio is small, the post-buckled panel weight can actually be reduced by increasing the stringer spacing provided other considerations such as pillowing and peeling stresses, damage tolerance, or noise transmission do not become critical.

Hoop Tension - Because of the very thin skin in the optimum pure compression panel designs, a nominal shear load ratio of 0.2 is chosen as a baseline for comparison of the remaining design parameters.

Hoop tensile loading reduces the weight of post-buckled panels due to its stabilizing effect on the stringer and due to increased effective longitudinal stiffness of the post-buckled plate. This effect is shown in Figure 22. Even a small hoop compressive loading, not shown, has the opposite effect of destabilizing the stringer reducing the skin longitudinal stiffness and increasing the panel weight.

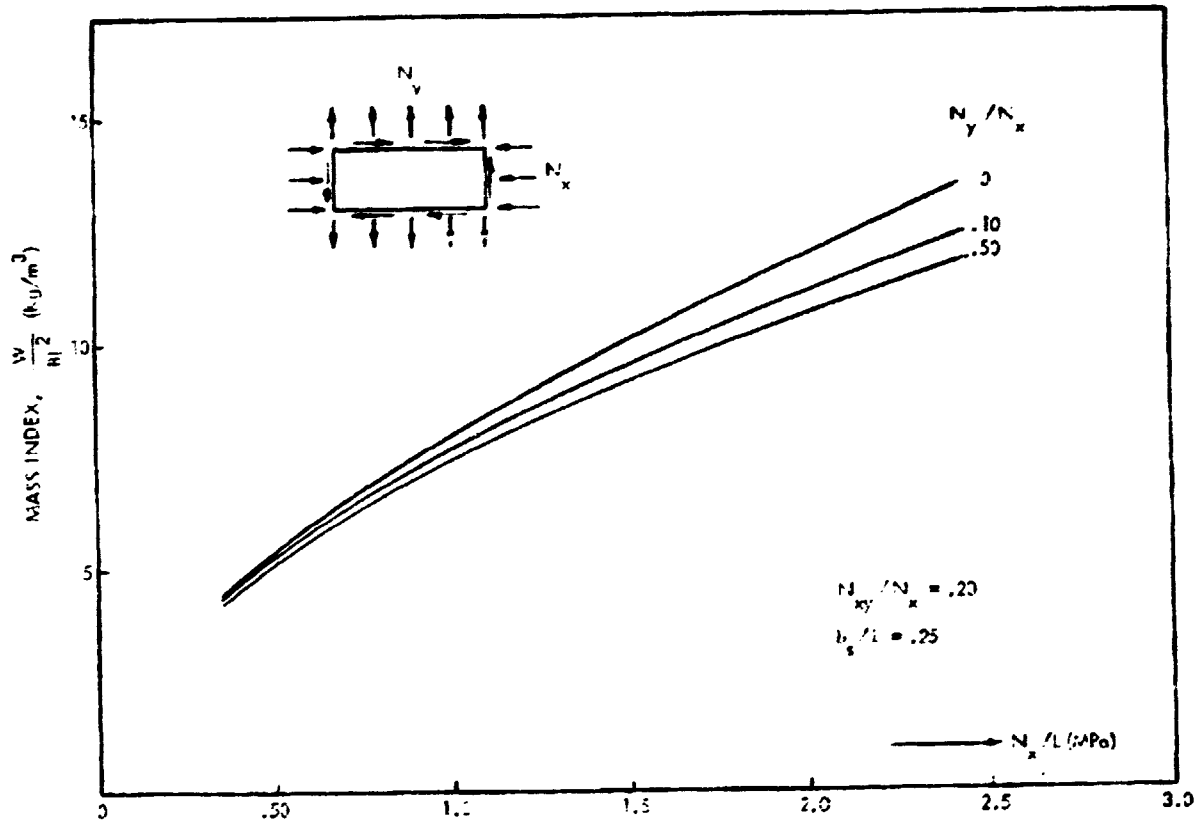

Figure 22. Effect of Hoop Tension on Panel Weight

Initial Eccentricities

Initial bow-type eccentricities, present in all real panels, increase the weight of post-buckled panels as shown in Figure 23. Values of e/L of not less than 0.001 should be considered and weight penalties of 5 to 10 percent may be expected. The major effect of this type eccentricity on the optimum panel is an increase in the stiffener height and the free flange width. The increase in stiffener height may in turn require an increase in the bending stiffness, D_{22}, of the web.

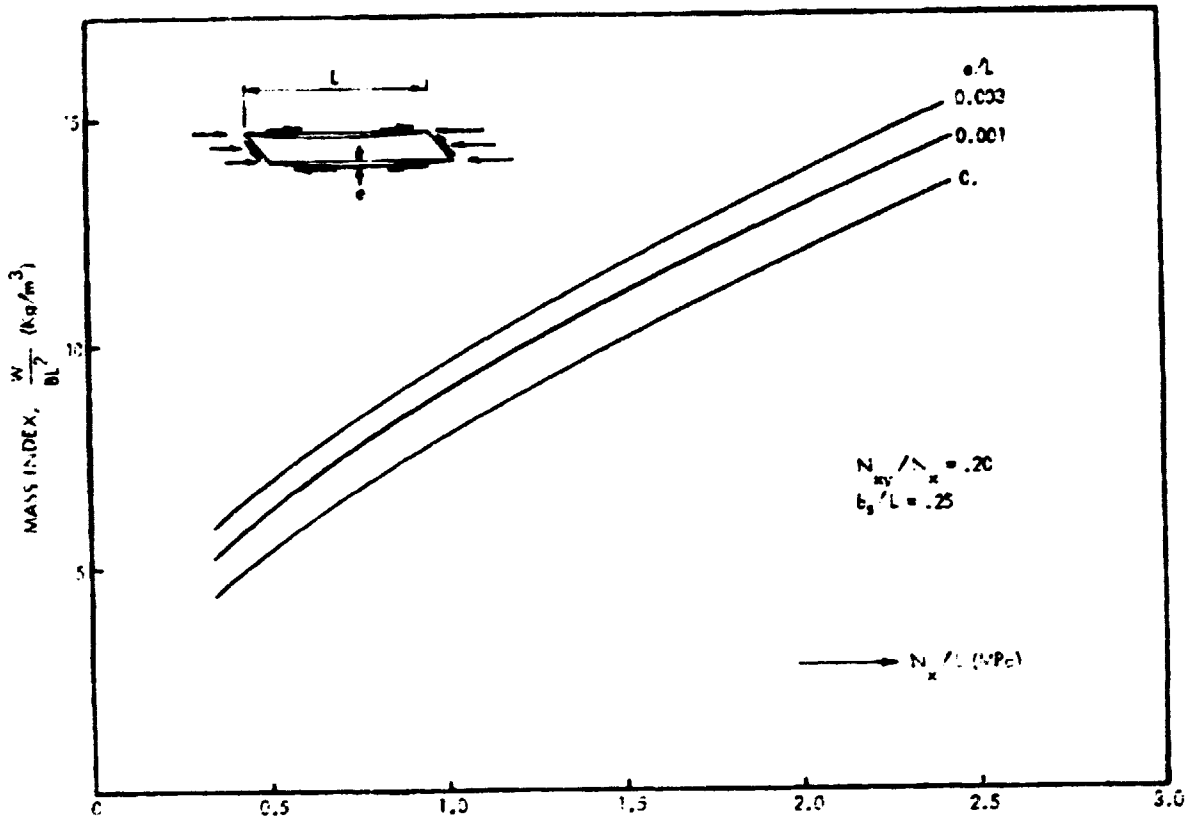

Figure 23. Effect of Initial Eccentricity on Panel Weight

Strain Limitation

If panel longitudinal and transverse membrane strains are limited to some value lower than the material strain limit, the panel weight will obviously increase. This effect is shown in Figure 24 for a strain limit of 0.004. The major variation in the designs required to achieve this limitation is an increase in the number of 0-degree plies in the stiffener free flange and the skin.

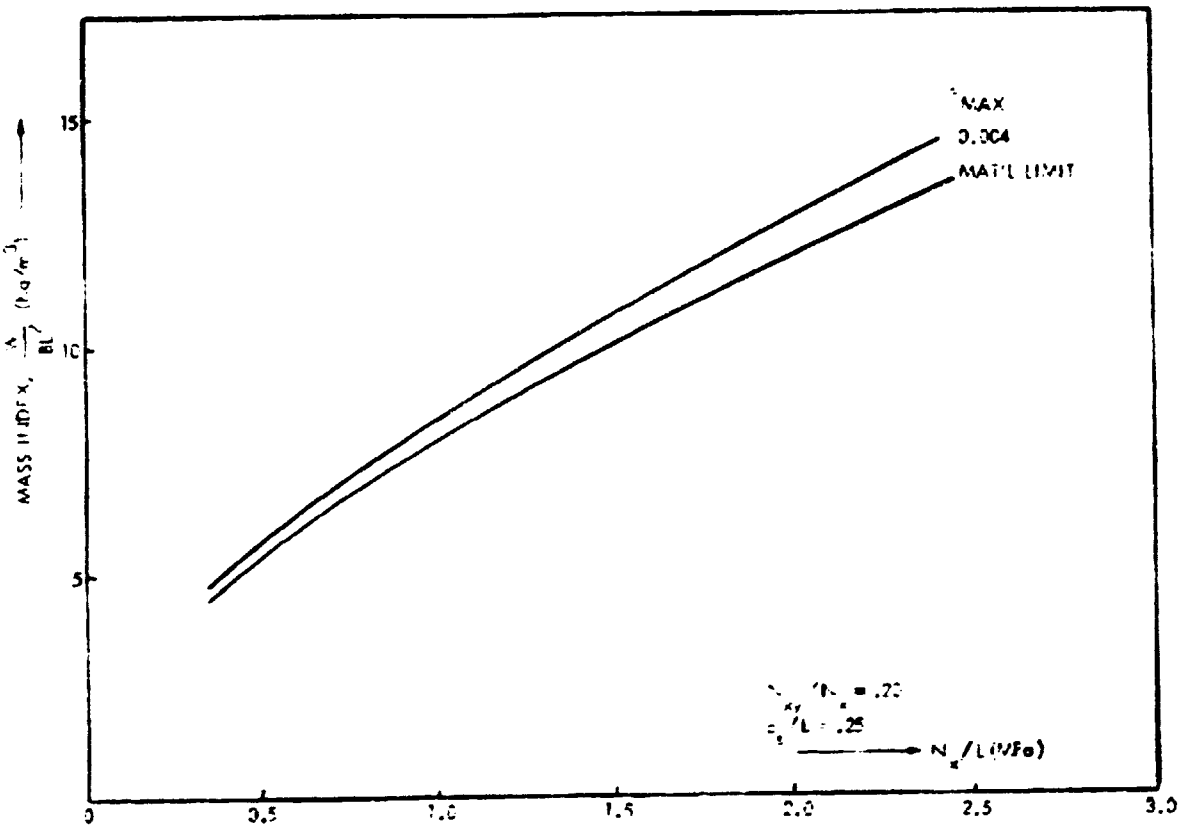

Figure 24. Effect of Strain Limitation on Panel Weight

Stiffener Cross-Sectional Shape

The shape of open stiffeners has only a very small effect on panel weight. Figure 25 shows that the blade-stiffened panels are only two percent heavier than the J- or I-stiffened panels. The effect of transverse shear flexibility, not considered in these results, could increase the penalty associated with blade stiffeners.

Final Post-Buckled Panel Sizing

J-shaped stiffeners were chosen for the final panel design since structural and nonstructural connections are greatly simplified when using the J- rather than I-shaped stiffeners. Previous studies have shown that these two stiffeners result in nearly equal weight optimum panels. Load condition number 2 of Table 4 proved to be the critical case with respect to stability. The panel was optimized for this loading with lower limits set on selected

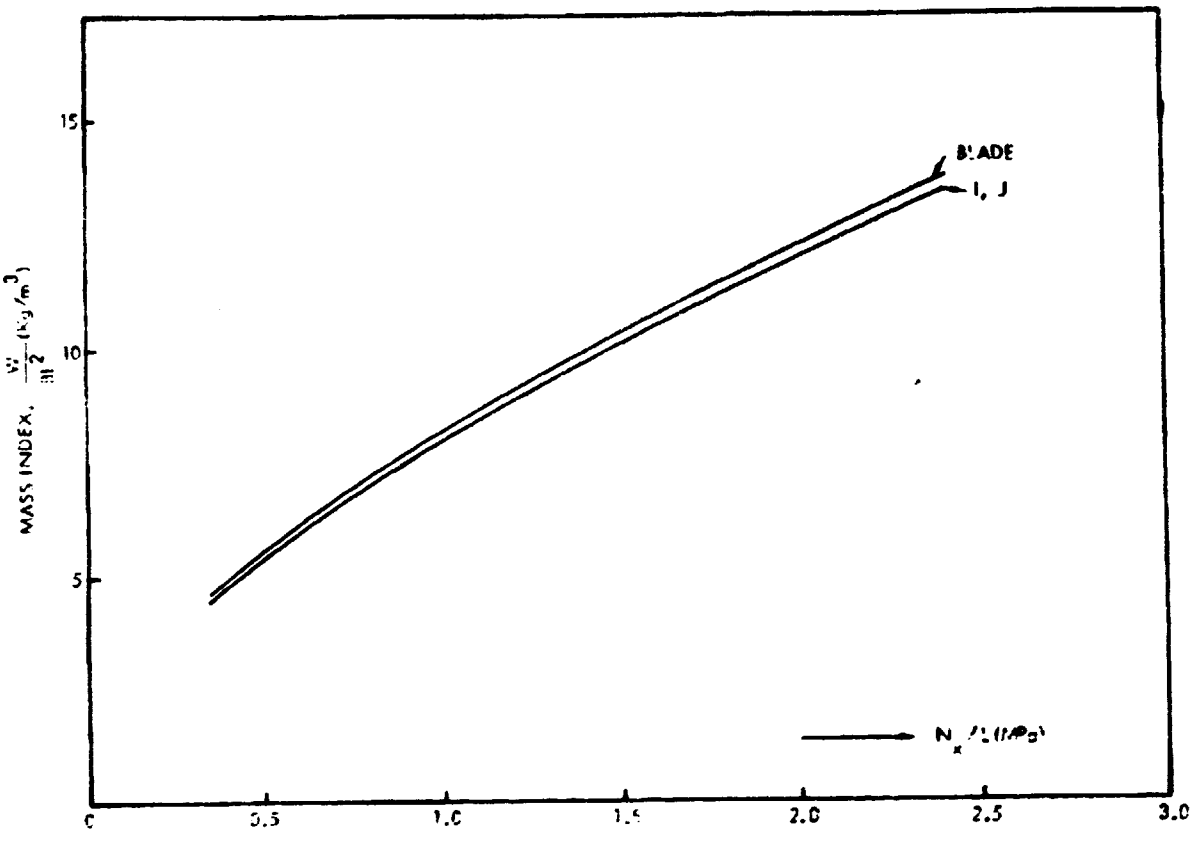

Figure 25. Effect of Stiffener Shape on Panel Weight

skin ply thicknesses so that conditions number 1 and 5 would not be critical. The adequacy of the panel under the other load conditions was then checked. An initial bow-type imperfection with a maximum eccentricity of 0.001 times the panel length was included. Damage tolerance membrane strain limitations of 0.0045 in tension and compression for both hoop and longitudinal strain were imposed.

The presence of hoop compression required single 90-degree plies on the outer surfaces of the skin. The minimum number of 45-degree plies was set at eight so that a shear stiffness similar to that of the L-1011 forward fuselage could be achieved. This last requirement was also necessary in order to satisfy imposed buckling criteria. Although the optimum number of 0-degree plies in the skin is in the range of four or five, it was decided to set this number at six to yield a 16-ply skin $[90/^{+}_{-}45/0_2/^{-}_{+}45/0]_S$ laminate. Further testing of composite panels under combined loading with emphasis on damage tolerance and stiffener/skin peeling could provide the confidence to utilize a thinner skin.

Due to the relatively small effect of stringer spacing on panel weight, an intermediate spacing of 14.7 cm (5.8 inches) was selected. With this spacing all buckling criteria are satisfied, and only two 90-degree plies are required to prevent wide column buckling of the skin between stringers due to external pressure.

Optimum J-stiffeners tend to be somewhat taller and have a thicker free flange than equivalent I-stiffeners. To keep the J-stiffener height reasonably small and, at the same time, to control the free flange thickness, it was decided to include at least two 0-degree plies in laminate 1 (Figure 18). An exterior 90-degree ply on the web provides resistance to stiffener rolling torsion. A total of eight 45-degree plies in the web was set as a practical minimum. In an attempt to improve the peel resistance of the panel, an additional 90-degree ply was included on the inner surface of laminate 1. This 90-degree ply matches the 90-degree ply on the skin and should improve the interface strength. Since it continues throughout the web, it also provides a tension tie-down link of the stringer to the skin. The effectiveness of this attempt to improve the stringer to skin bond will be evaluated in subsequent tests. The resulting web lay-up of $[90/\pm 45/0_2/\mp 45/90]_S$, while certainly not optimum with respect to weight, appears to be a good solution with respect to the practical considerations discussed above. An additional nonoptimum factor is the inclusion of two 90-degree plies in laminate 2 of this free flange so that there are no more than six adjacent 0-degree plies. The mass index of the final skin-stringer panel is 10.7 kg/m^3.

FINAL DESIGN ANALYSES

Panel Configuration

The final composite panel design, shown in Figure 26, is structurally representative of a wide-bodied pressurized fuselage. The panel, which is fabricated entirely of graphite/epoxy material, has a length of 152.4 cm (60.0 inches) and is 101.6 cm (40.0 inches) wide. While minimum weight considerations dictated the sizing of the basic skin-stringer panel, the spacing, geometry and stiffness of the frames used in the design correspond to those used on the L-1011 forward fuselage. Details such as shear clips and attach-

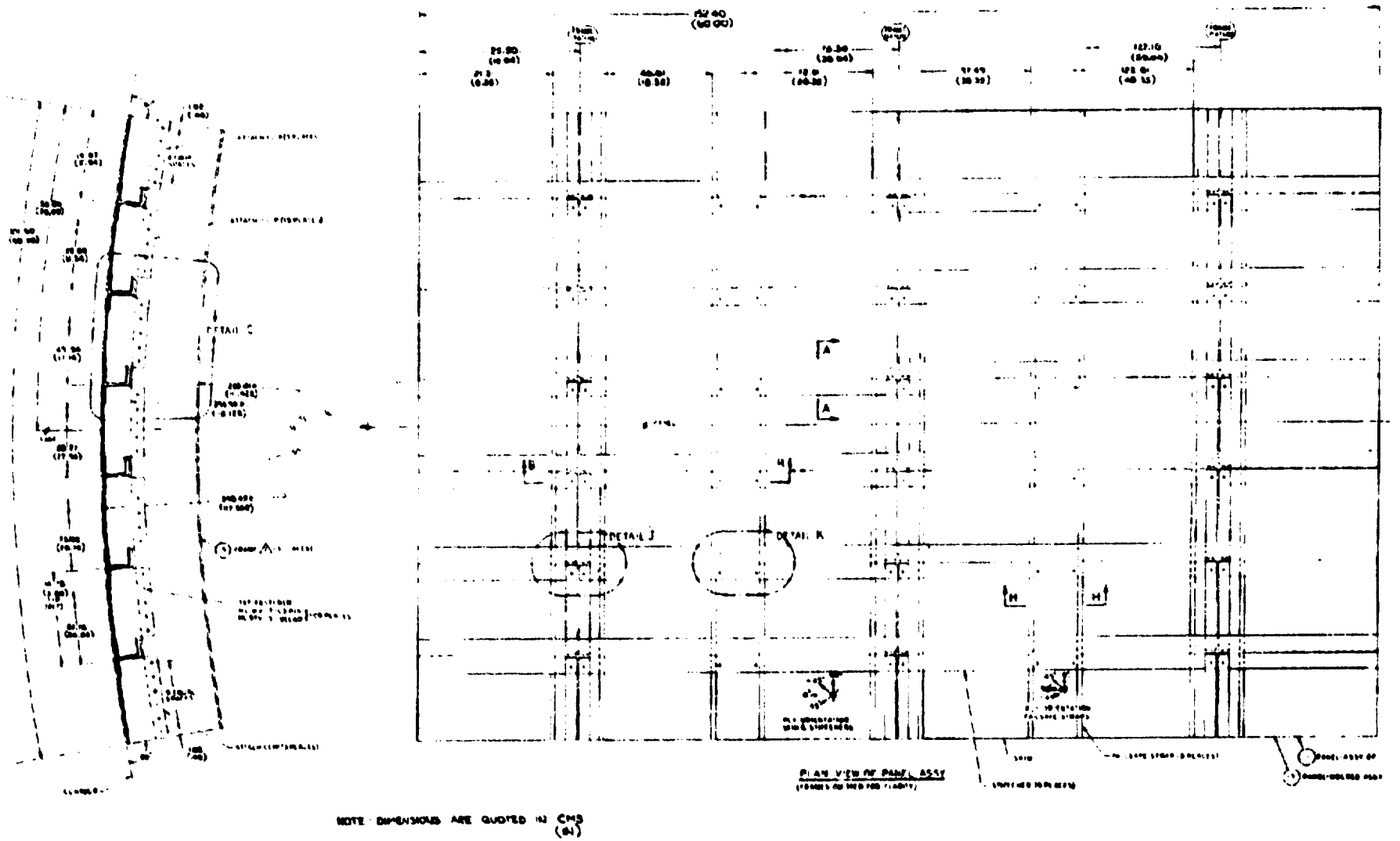

Figure 26. J-Stiffened Curved Panel Assembly (Sheet 1 of 2)

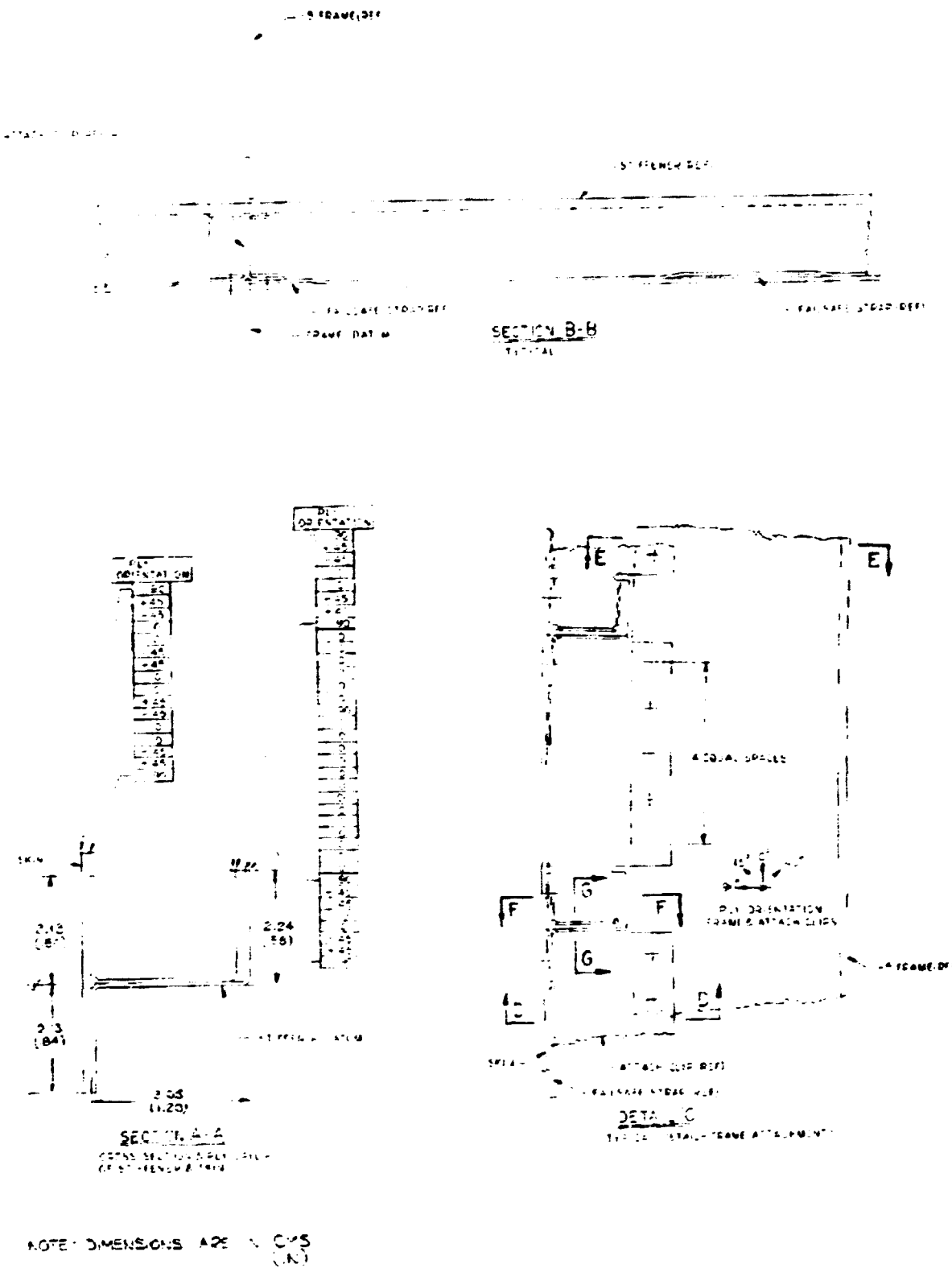

Figure 26. J-Stiffened Curved Panel Assembly (Sheet 2 of 2)

ments were influenced to a large degree by the desire to fabricate this component as economically as possible with respect to both minimizing the number of bond cycles and reducing conventional assembly methods. This has been accomplished through a design which allows the skin, stringers, frames and fail-safe straps to be molded in a single operation, limiting the use of mechanical attachments to the assembly of pre-cured frame members.

Fail-safe straps are provided at all frame and mid-bay locations. Being comprised of six plies of unidirectional tape, these straps are to serve the dual function of an effective crack stopper and provide an alternate load path in the event of a skin failure. Also, the straps at frame locations are utilized as additional frame cap material.

A detail of a typical stringer is shown in Section A-A, Figure 26. The J-section configuration was selected as offering the best compromise when considering structural efficiency and ease of manufacturing. The double flange attachment to the skin, while increasing the complexity of ply lay-up, provides a much stronger joint, which is necessary to prevent separation of skin and stiffeners in the post-buckling range. Stringers run continuously the full length of the panel with the skin attachment flange being joggled at all fail-safe strap locations. (See Section B-B, Figure 26.)

Although it is technically feasible to integrally mold frame members together with the skin panel, the complexity of such a holding fixture would have been significantly increased and little or no structural improvement will be realized. Alternate methods of frame attachment were therefore studied with the concept shown in Detail 'C' of Figure 26 being ultimately selected.

It will be noticed that anti-peel fasteners have been added in all areas where there is a tendency to have a tension load on the bond line.

Pressurized Shell Analysis

A Lockheed in-house computer program for the analysis of composite circular cylindrical shells, stiffened by equally spaced rings and stringers, subjected to uniform pressure is used to determine local strains, displacements and stresses. These local strains and stresses are caused by the restraining effect of the rings or frames and, to a lesser extent, by that of the

stringers. This is commonly referred to as "pillowing" of the skin. The stiffeners are treated as separate components which are coupled with the skin through interacting normal and shear loads. Inasmuch as the cross section of the stiffeners are considered nondeformable, the interacting stresses between the skin and stiffener flange are assumed to be uniform across the flange width.

An analysis was made for the ultimate ground test condition in which the shell is subjected to an internal pressure of 0.1215 N/M^2 (17.63 psi). Numerical results for the inner and outer surface strains at various locations on the shell are presented in Figures 27 and 28. The solid lines in these figures represent variations along a line midway between adjacent rings (x = 0), and the dashed lines show the variations along a line midway between adjacent stringers (y = 0). It is clear that the difference between outer and inner surface strains indicate the extent of curvature change of the skin which is related to the bending of the skin.

As shown by the solid lines in Figure 27, the change in curvature in the longitudinal direction for points along x = 0 is insignificant. The maximum curvature change in the longitudinal direction occurs at the ring location. The corresponding curvature change in the circumferential direction, as shown in Figure 28, is negligibly small, as is to be expected. Although the maximum curvature change in the circumferential direction occurs at the stringer location, that at the point midway between adjacent rings and stringers (0,0) is also significant, as shown in Figure 28. As anticipated, the mean value of the strain (membrane strain) in the circumferential direction is much larger than that in the longitudinal direction.

To evaluate closer the interacting normal stress between the skin and stiffener flange, an analysis based on beam theory has been made. The adhesive or interlayer is modeled as a series of parallel springs. Transverse shear and moment at selected locations calculated from the general stiffened shell analysis are used as applied loads in the skin along the free edge of the flange. The normal stress distribution between the skin and stringer at x = 0, and between the skin and ring at y = 0, are presented in Figure 29. It is seen that sharp stress gradients occur near the free edge of the flange.

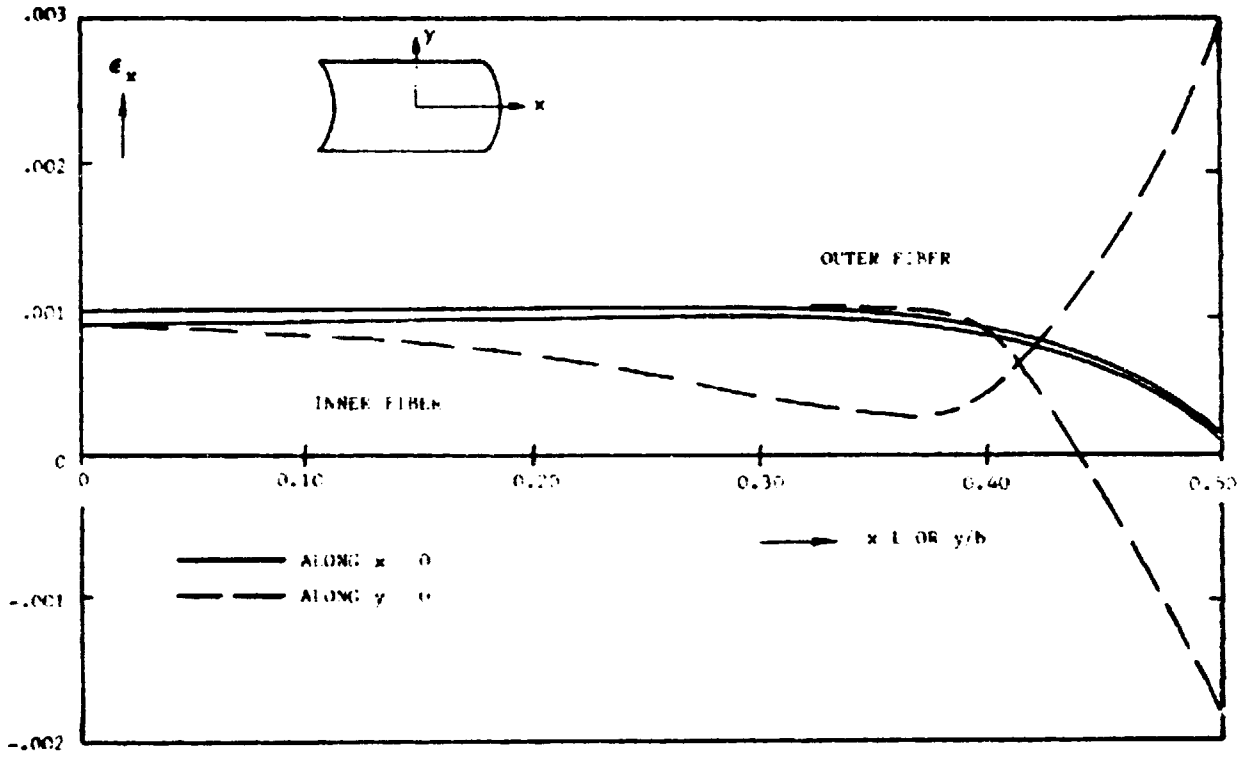

Figure 27. Longtitudinal Strains Due to Skin Pillowing

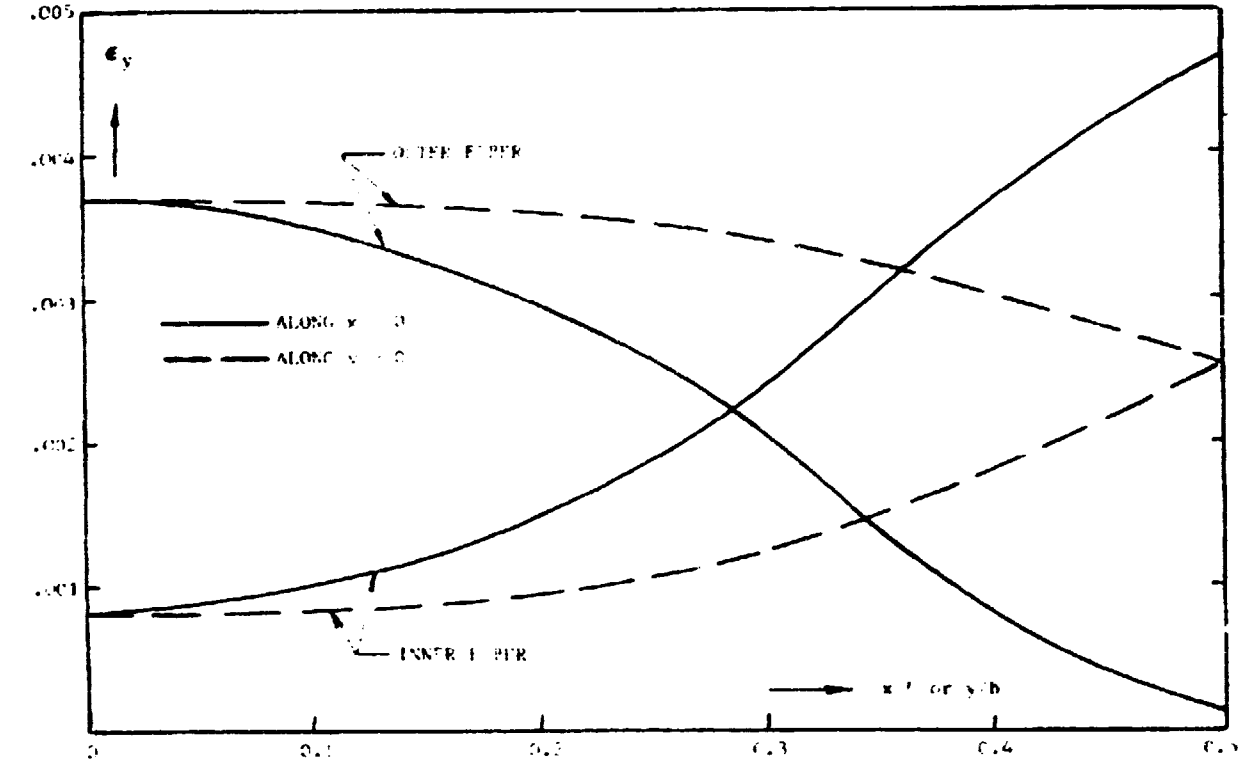

Figure 28. Transverse Strains Due to Skin Pillowing

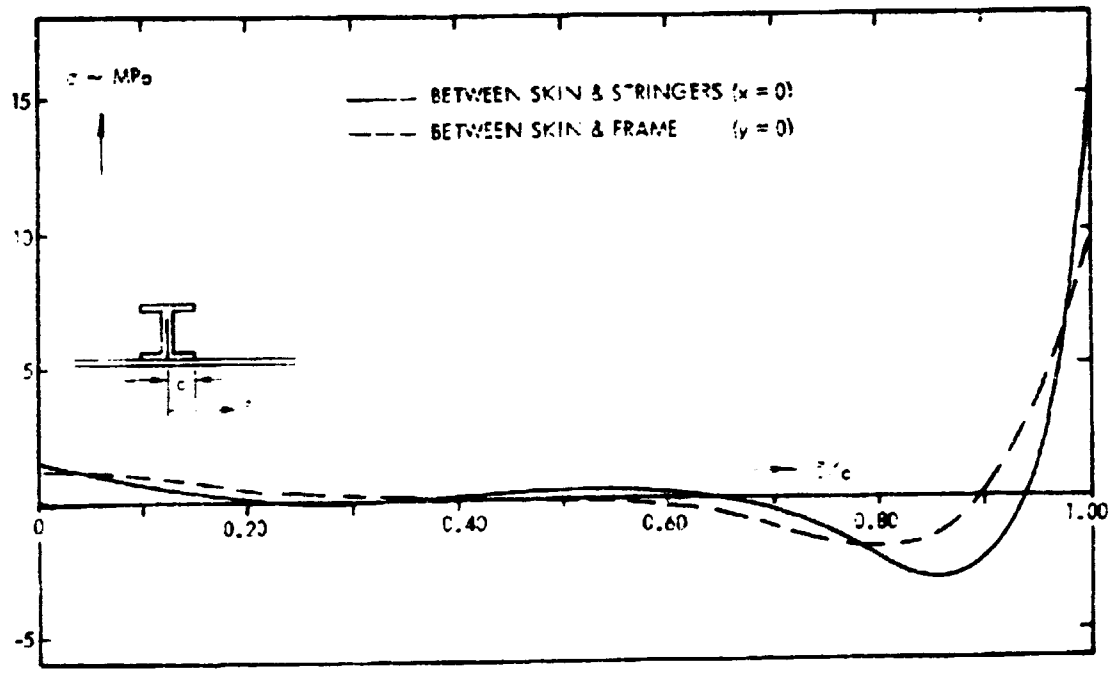

Figure 29. Interacting Normal Stress Between Skin and Stiffeners

Fail-Safe Analysis

In a typical large pressurized composite fuselage, skin panels are formed to the required skin curvature together with longitudinal stringers and circumferential frames. To prevent the longitudinal propagation of damage, circumferential fail-safe straps are positioned on the inside of the skin at each frame station and, in many cases, midway between frames. To be effective, adjacent mid-bay straps must be capable of containing the damage resulting from complete and sudden loss of all structure between them, including the frame.

This problem has been investigated under Lockheed-funded IRAD projects in fracture mechanics and structural integrity of composites. The analysis and results are described below

Analysis Procedure and Results

The analysis was based on the assumption of a severed frame and fail-safe strap and a skin crack extending 21.6 cm (8.5 inches) in both directions to the adjacent mid-bay straps. The panel was treated as a flat panel subjected

to static tension only. The K_c concept (fracture toughness) was chosen as the fracture criterion, i.e.

$K < K_c$; Crack arrest or no fracture

$K \geq K_c$ Fracture occurs

where K is the stress intensity factor. The fracture toughness, K_c, was estimated at 36.8 MPa $\sqrt{m}$ (33.5 ksi $\sqrt{in.}$) for this case, based on available Lockheed data.

The geometry considered in the analysis is shown in Figure 30. It consists of a 16-ply $[90/\pm45/0_2/\mp45/0]_S$ skin panel with two 7.62 cm (3.0-inch) wide fail-safe straps. The latter is made of six plies of unidirectional graphite/epoxy material. A through-the-thickness crack was assumed in the geometric center of the panel. A finite element method which included an anisotropic crack-tip element (Reference 7), developed at the Lockheed-Georgia Company, was used to analyze the structure.

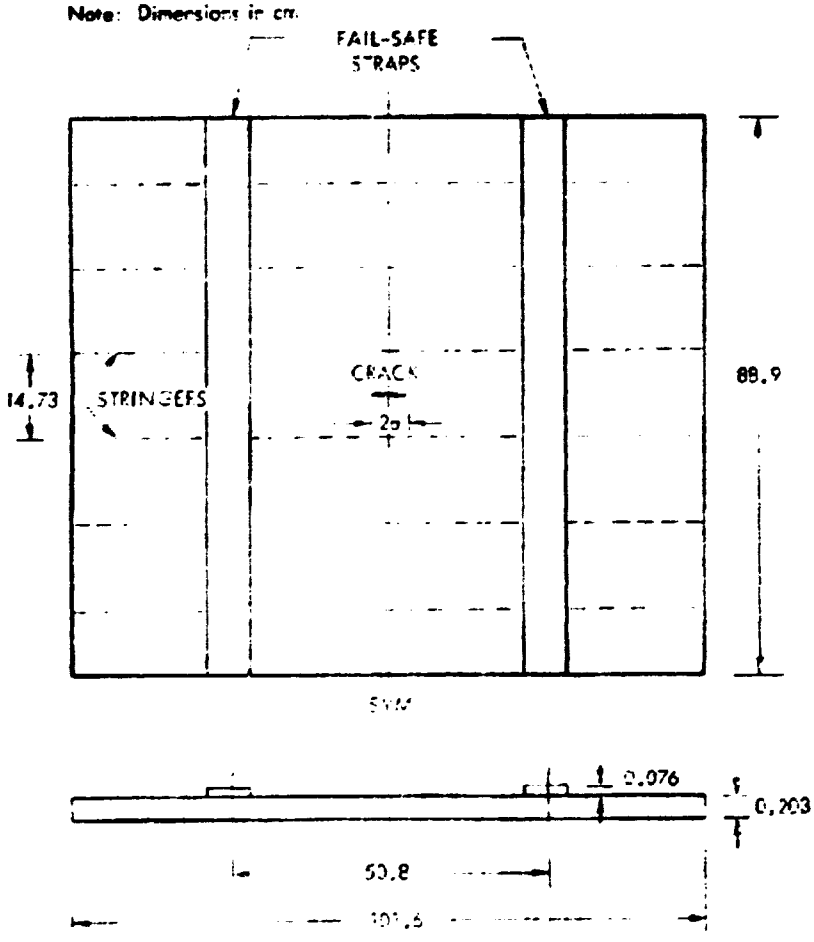

Figure 30. Analysis Geometry

The finite element model, as shown in Figure 31, consists of anisotropic triangular and quadrilateral elements representing the skin panel and fail-safe straps, and one eight-node anisotropic cracked element (Figure 32), representing the crack-tip. Linear shear spring elements were used to represent the interface between the straps and skin panel. The model was subjected to a remote stress field of 82.7 MPa (12.0 ksi) which corresponds to an applied internal pressure of 0.058 N/m^2 (8.4 psi). Successive delamination of the interface layer, caused by crack growth, was considered in the analysis.

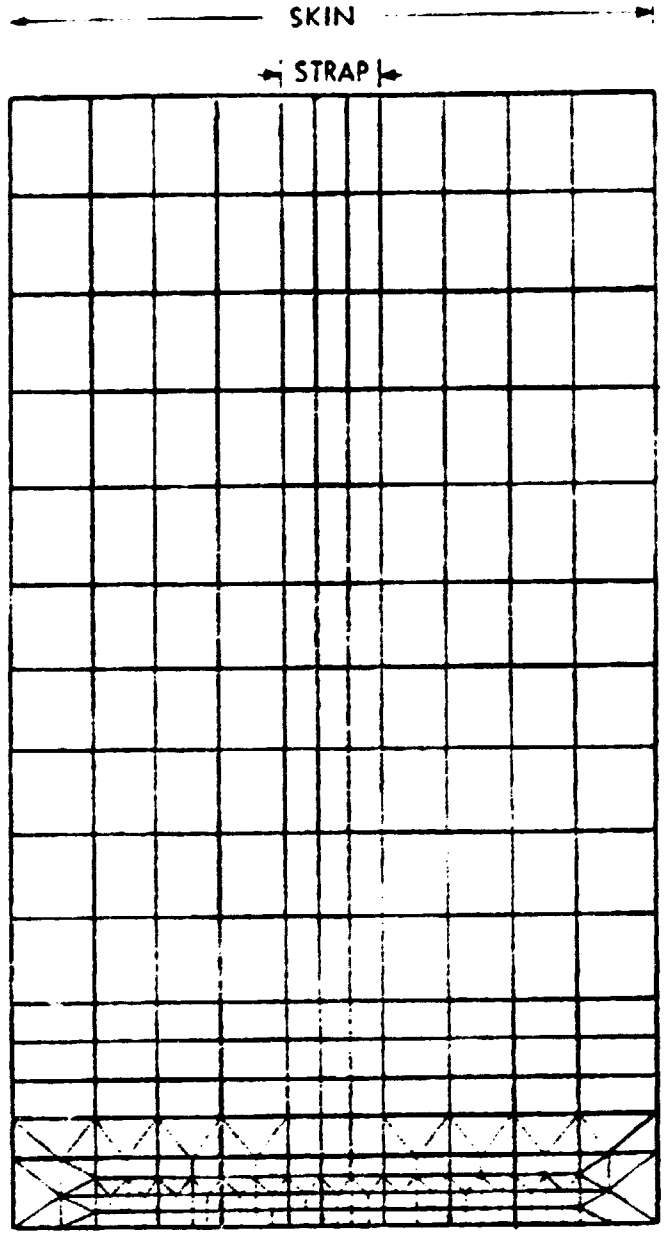

Figure 31. Finite Element Model

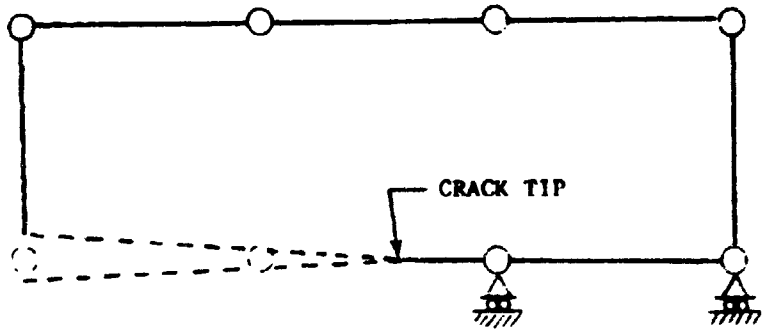

Figure 32. Eight-Node Anisotropic Cracked Element

As the crack advanced in the model, the shear springs were monitored and automatically released when the spring force reached its ultimate strength. This simulates local delamination at the interface between skin and strap.

The computed stress-intensity factors (K), as shown in Figure 33, are lower than for the skin panel without straps, even before the crack reaches the strap. A further reduction in the stress-intensity factor can be obtained as the crack grows beneath the strap. However, when the crack approaches the end of the strap area, the K value again tends to increase. As seen from Figure 33, no fracture will occur if the fracture toughness (K_c) of the skin material exceeds approximately 67.0 MPa $\sqrt{m}$ (61 ksi $\sqrt{in.}$). It should also be noted that no crack arrest will occur if the K_c value is lower than 29.7 MPa $\sqrt{m}$ (27 ksi $\sqrt{in.}$). Between these two extremes, unstable crack growth will occur and the crack will be arrested as long as the strap is intact.

For the estimated K_c = 36.8 MPa $\sqrt{m}$ case, it is seen that unstable crack growth will occur at Point A in Figure 23 and will be arrested at Point B. In other words, the critical crack length under an 82.7 MPa far field stress will be about 15.2 cm (6.0 inches) and this crack can be arrested at the strap location.

The residual strengths were computed using the estimated K_c value. The results are plotted in Figure 34. Assuming an existence of a 15.2 cm crack, the load can be applied to Point A without causing an increase in the crack length. At Point A, the crack extends to Point B without any load increase; this is the point of crack arrest. In the case of a load increase only, the crack propagates until it reaches Point C, corresponding to the load carrying

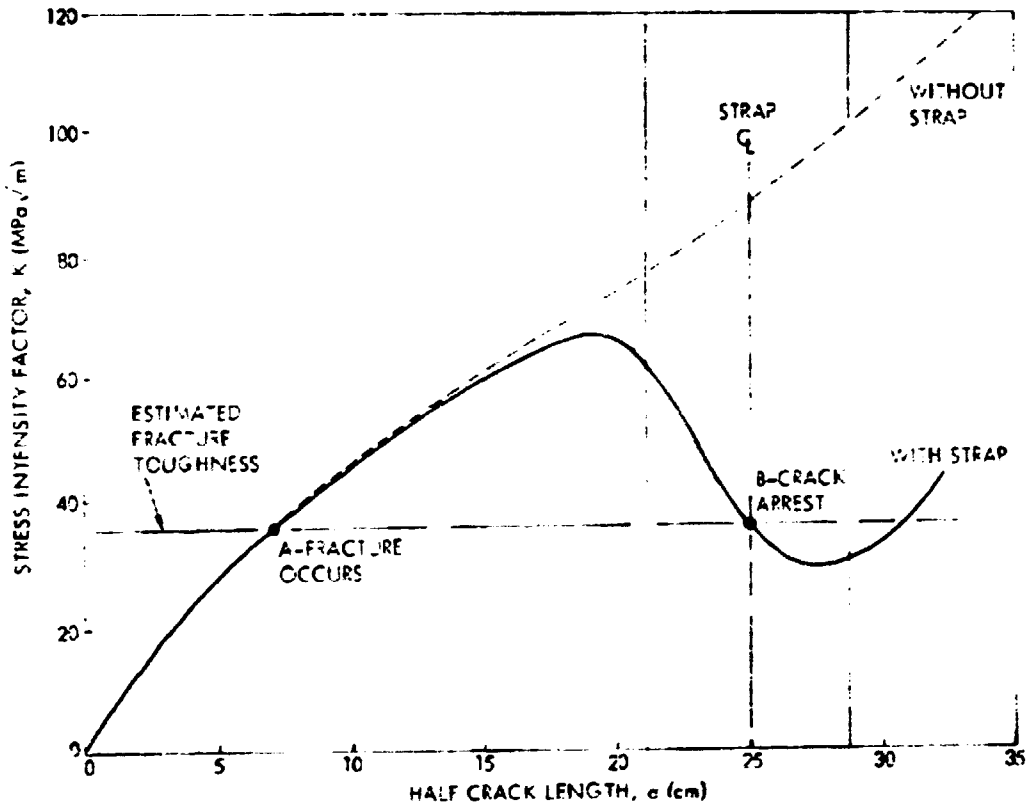

Figure 33. Stress Intensity Factor versus Half Crack Length

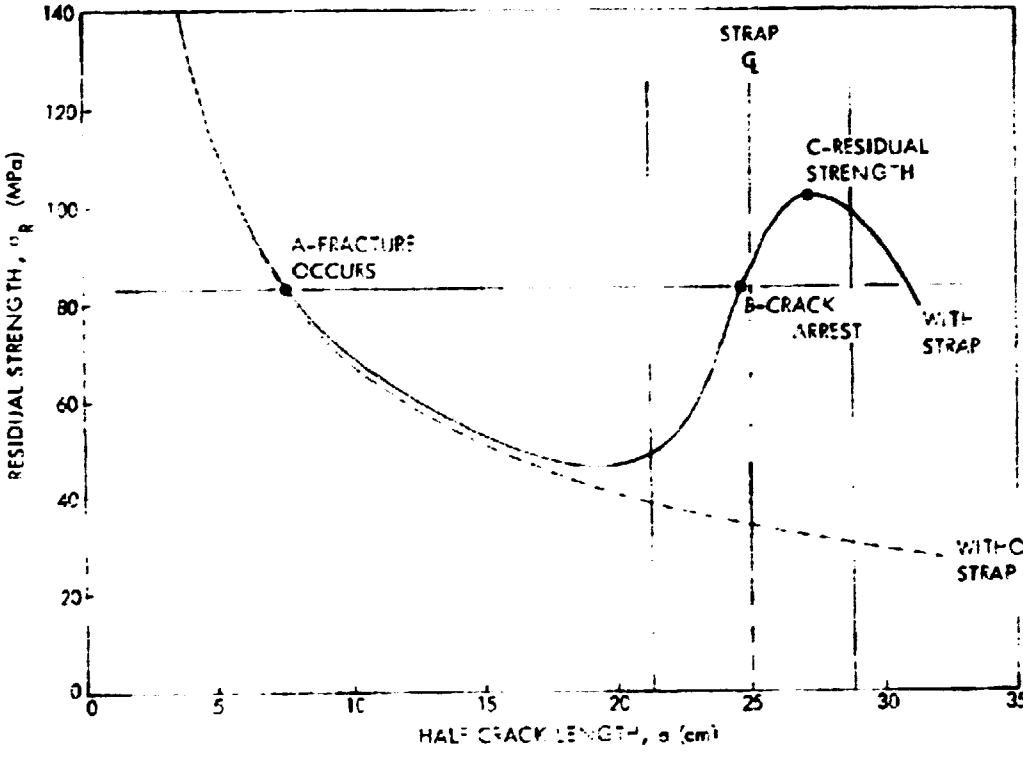

Figure 34. Residual Strength versus Half Crack Length

capacity (residual strength) of the structure after crack arrest. For the panel without a strap, failure occurs at Point A without any mechanism to stop the running crack. Furthermore, no residual strength can be obtained.

Figure 35 shows both average and maximum stresses in the strap. The maximum stress occurs at the strap edge facing the approaching crack. The results indicate that the stresses in the strap are lower than its ultimate tensile strength and no strap failure would occur for the crack length considered.

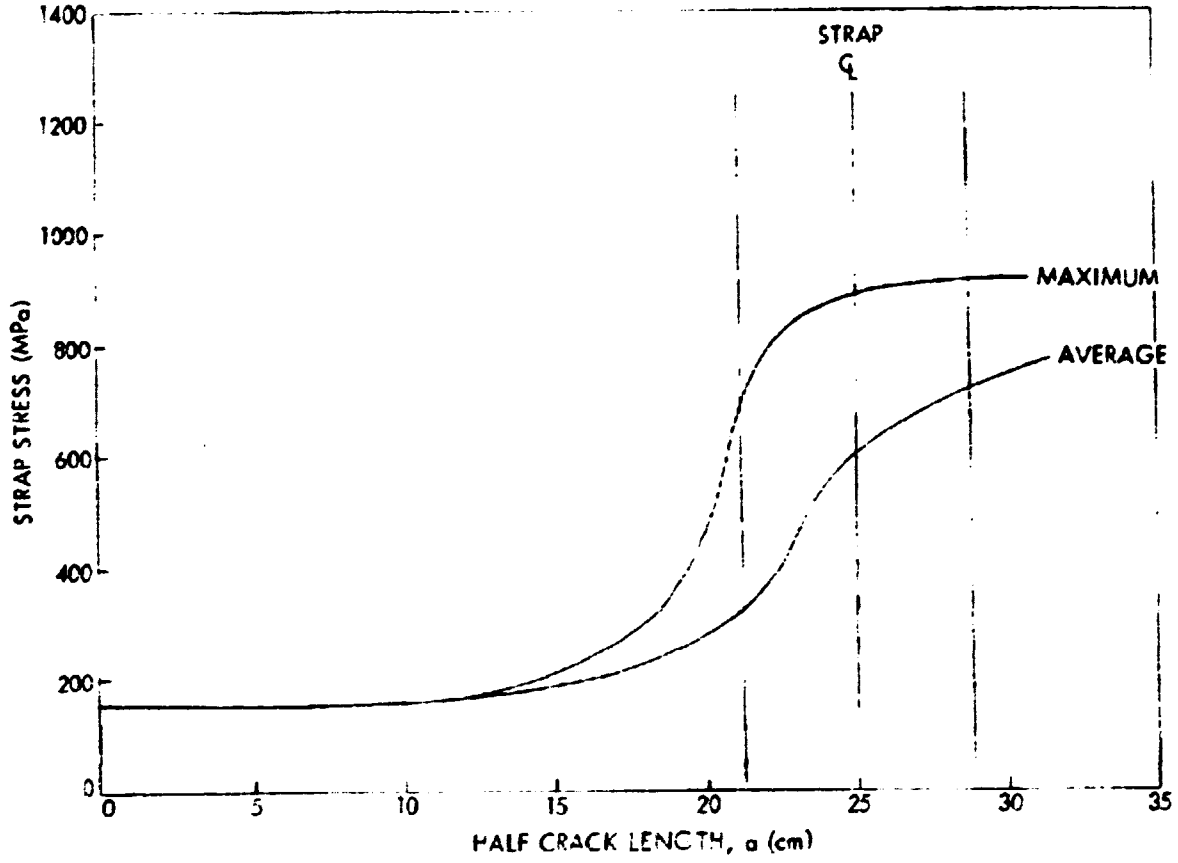

Figure 35. Stress in Fail-Safe Strap

CONCLUDING REMARKS

A stiffened composite panel has been designed based on loads and criteria representative of the forward fuselage of a typical commercial transport aircraft. The panel is a minimum weight design, constrained by practical manufacturing considerations and fatigue and damage tolerance requirements. The final configuration is an all graphite/epoxy panel with longitudinal J-stiff-

eners in which the skin between adjacent stiffeners is permitted to buckle under design loads.

It has been shown that significant weight savings are obtained with post-buckled design for the stiffener spacings considered. An additional benefit of post-buckled skin design is the relatively small weight penalty associated with an increase in stringer spacing when compared to that incurred in buckling resistant design. The latter results in fewer parts which can be translated directly into reduced cost.

Initial bow-type eccentricities are included in the analysis in order to account for manufacturing tolerances and other imperfections which are always present in real panels. Weight penalties of from 5 to 10 percent may be expected in practical design.

Local strains and stresses caused by the restraining effect of rings or frames and stringers were evaluated for the final panel design. These local strains or stresses are generally not a critical design condition but may dictate the number of 90-degree plies in the skin.

Damage tolerance is a major concern in pressurized composite fuselage design. Design strain levels are currently restricted by many considerations including tolerance for impact damage. In the present design, 7.62 cm wide fail-safe straps are positioned on the inside of the skin at each frame and midway between frames in order to prevent the longitudinal propagation of damage. A finite element analysis was performed to evaluate the crack arrest capability and residual strength of the structure.

Additional theoretical and experimental work must be performed in order to investigate the behavior of post-buckled structure. One specific problem is the separation of skin and stiffeners caused by out-of-plane displacements when the stiffeners are co-cured or bonded to the skin.

REFERENCES

1. Davis, G.W. and Sakata, I.F., Design Considerations for Composite Fuselage Structure of Commercial Transport Aircraft, NASA CR-159296, August 1980.

2. Vanderplaats, G.N.: The Computer for Design Optimization, Computing in Applied Mechanics, AMD-Vol. 18, ASME Winter Annual Meeting, New York, December 1976.

3. Koiter, W.T.: Het Schuifplooiveld by Grote Overschrydingen van de Knikspanning, NLL Report S295, November 1946.

4. Anderson, M.S., et al: PASCO: Structural Panel Analysis and Sizing Code - Users' Manual, NASA TM-80182, January 1980.

5. Williams, J.G., et al: Recent Developments in the Design Testing and Impact Damage Tolerance of Stiffened Composite Panels, NASA TM-80077, April 1979.

6. Williams, J.G.; Stein, M.: Buckling Behavior and Structural Efficiency of Open-Section Stiffened Composite Compression Panels, AIAA/ASME/SAE 17th SDM Conference, Valley Forge, Pennsylvania, May 1976.

7. Chu, C.S., et al:; Finite Element Computer Program to Analyze Cracked Orthotropic Sheets, NASA CR-2698, July, 1976.

1. Report No.	2. Government Accession No.	3. Recipient's Catalog No.
NASA CR-159302		

4. Title and Subtitle	5. Report Date
Design and Analysis of a Stiffened Composite Fuselage Panel	August 1980
	6. Performing Organization Code

7. Author(s)	8. Performing Organization Report No.
J.N. Dickson and S. B. Biggers	LG80ER0137
	10. Work Unit No.

9. Performing Organization Name and Address	11. Contract or Grant No.
Lockheed-Georgia Company Marietta, GA 30063	NAS1-15949
	13. Type of Report and Period Covered
12. Sponsoring Agency Name and Address	Contractor Report
National Aeronautics and Space Administration Washington, DC 20546	14. Sponsoring Agency Code

15. Supplementary Notes Langley technical monitor: James H. Starnes, Jr. (Topical Report)
Use of commercial products or names of manufacturers in this report does not constitute official endorsement of such products or manufacturers, either expressed or implied, by the National Aeronautics and Space Administration.

16. Abstract

A stiffened composite panel has been designed that is representative of the fuselage structure of existing wide bodied aircraft. The panel is a minimum weight design, based on the current level of technology and realistic loads and criteria. Several different stiffener configurations were investigated in the optimization process. The final configuration is an all graphite/epoxy J-stiffened design in which the skin between adjacent stiffeners is permitted to buckle under design loads. Fail-safe concepts typically employed in metallic fuselage structure have been incorporated in the design. A conservative approach has been used with regard to structural details such as skin/frame and stringer/frame attachments and other areas where sufficient design data was not available.

17. Key Words (Suggested by Author(s))	18. Distribution Statement
Composites Fuselage Stiffened Panels Postbuckling Structural Optimization Failsafe	Unclassified - Unlimited Subject Category 39

19. Security Classif. (of this report)	20. Security Classif. (of this page)	21. No of Pages	22. Price*
Unclassified	Unclassified	50	A03

* For sale by the National Technical Information Service, Springfield, Virginia 22161

END

FILMED

DTIC